2009

# Optimal Design of Passive Fluid Viscous Dampers for Controlling Vibrations in Seismically-Excited Truss Towers

Sujatha Kalyanam

FLORIDA STATE UNIVERSITY

COLLEGE OF ENGINEERING

# OPTIMAL DESIGN OF PASSIVE FLUID VISCOUS DAMPERS FOR CONTROLLING VIBRATIONS IN SEISMICALLY-EXCITED TRUSS TOWERS

By

SUJATHA KALYANAM

A Thesis submitted to the
Department of Civil and Environmental Engineering
in partial fulfillment of the
requirements for the degree of
Master of Science

Degree Awarded:
Summer Semester, 2009

The members of the Committee approve the Thesis of Sujatha Kalyanam defended on May 5, 2009.

_____
Michelle Rambo-Roddenberry
Professor Directing Thesis

_____
Lisa Spainhour
Committee Member

_____
Sungmoon Jung
Committee Member

Approved:

_____
Kamal Tawfiq, Chair, Department of Civil and Environmental Engineering

_____
Ching-Jen Chen, Dean, College of Engineering

The Graduate School has verified and approved the above named committee members.

I dedicate this manuscript to my husband for his utmost support and patience through this whole process.

## ACKNOWLEDGEMENTS

I wish to acknowledge and thank Dr. Ken Walsh for his unwavering support and guidance throughout the length of the research that led to this thesis. I wish to thank Dr. Michelle Rambo-Roddenberry for her support as a mentor and advisor. I also wish to thank my committee members, Dr. Lisa Spainhour and Dr. Sungmoon Jung, for their time and guidance.

## TABLE OF CONTENTS

## LIST OF TABLES

## LIST OF FIGURES

## ABSTRACT

Truss towers form a vital part of the communication infrastructure, and the control of responses for such structures during adverse events such as an earthquake is of significant importance. The objective of this research venture is to combine the linear quadratic regulator (LQR) algorithm for optimal design of supplemental dampers of buildings with the bi-model method for a truss tower. Damping coefficients are calculated for the 3D truss model by analyzing the dynamically equivalent 2D lumped mass model which is developed using the bi-model method. The dynamic responses of the structure for given seismic loads are computed for the conditions with and without dampers. The results are then compared to determine the efficiency of the method to design passive fluid viscous dampers (PFVD) to control the excess vibrations due to seismic loads in towers.

# 1.0 INTRODUCTION

Towers are typically used for communication and can be classified based on their structural action as monopole towers, guyed towers, and lattice/truss towers. In this research venture the focus is on truss towers. These towers are typically three-sided with a triangular base and are supported on the ground or on buildings. They are flexible and often used in heavy loading conditions. Though they are heavy structures, they require very little base area. The control of excess vibrations due to adverse conditions such as an earthquake is essential because truss towers form an integral part of the communication infrastructure and their proper functioning is paramount to such situations.

Control of excess vibration of existing truss tower structures due to dynamic loads is a challenging and constantly evolving subject to civil engineers. Various techniques have been presented by researchers on this topic. The systems for control of vibrations of structures can be broadly classified into three groups: (1) active control system which requires external energy in the form of a large power source to function, (2) semi-active control system which requires external energy in the form of a small power source to function, (3) passive control system which does not require any external energy source to function. For passive control devices, the control forces are developed based on the response of the structure at the point of location of the control system [1]. The focus of this research is on passive control systems/devices and in particular the passive fluid viscous damper (PFVD).

The conventional approach for structures to resist the harmful effects of earthquakes passively is through strength, deformability and energy absorption [2]. Damping level is typically low in these structures and hence the low energy dissipation when within elastic range. One way to approach the resistance of structures to strong earthquakes is by installing a PFVD as a supplemental energy dissipation system instead of relying on the structure itself to dissipate the earthquake energy. In fluid dampers, the energy dissipation occurs through the conversion of mechanical energy to heat energy through deformation of the viscous fluid [3]. In these devices the piston acts to not only deform the fluid but also force it out through small orifices thereby

leading to great levels of energy dissipation. This high energy dissipation density of the fluid results in physically compact dampers making them suitable for applications in civil engineering structures.

Extensive work has been done on exploring the effect of PFVD in controlling the response of buildings to dynamic loads [4]. The authors of [5] presented work on various passive energy dissipation devices one of which was the PFVD. They observed that this supplemental damper not only offered notable control of the structure's drift for seismic loads, but also the reduction in base shear. They also noted the insensitivity of the fluid for a wide range of temperatures hence making it more reliable under extreme weather conditions. The authors of [6] have presented the efficiency of motion amplification device with PFVD in a toggle brace damper system. These devices amplify a small interstory drift to amplify the stroke of the damper. They observed that the PFVD's effectiveness was related to the stiffness of the braces in the toggle brace damper system. They noted that if the braces were very stiff then the damper acted in its full capacity. The same was observed by Constantinou [7] and Taylor [8]. Similarly, the authors of [9] have presented results on the effectiveness of PFVD with toggle bracing mechanism in controlling the vibration of a three-story frame model. They compared this with the response of buildings with only diagonally placed PFVDs. The observed that while there is no single rule to positioning the dampers on a structure, the toggle bracing of the dampers proved to be more efficient in reducing the interstory drift. The authors of [10] suggest a method to reduce the response of the structure due to seismic loads using viscous dampers with their effect magnified with mechanical levers. They observed that this method yielded much higher energy dissipation and reduced the peak displacements with no significant change in base shear. The authors of [11] obtained a semi-empirical design equation for a doubly acting PFVD to determine the damping material and size. They conducted experiments and observed good agreement between the theoretical and experimental results. A PFVD with magnetorheological was conceived by the authors of [12]. They observed that this device behaved as a linear viscous damper under smaller vibrations and behaved like a variable force damper under larger vibrations.

The design of a PFVD in a non-arbitrary way to best reduce the response of structures to dynamic loads is of great interest. The authors of [13] present guidelines for design of PFVD based on the elasticity of the structure. They observed that the PFVD's are most effective for elastic structures in the range of natural periods and not as effective for long-period inelastic structures. The authors of [14] have presented techniques to calculate the damping coefficients of supplemental PFVD's for each floor of a ten-story structure using the linear quadratic regulator (LQR) algorithm. They concluded that this is both cost-effective and the damper capacity is proportional to the stiffness of the building. In a similar effort the authors of [15] have presented various techniques to design supplemental dampers for multistory structures using LQR algorithm. One of the techniques that they presented to calculate the optimal damping coefficients for PFVD is the single mode estimator approach which is based on active control theory. They concluded that this design solution is always stable as the formulation is based on the algebraic Riccati equation (ARE). They also observed that since the method was based on active control, the equivalent effect can be achieved only by passive devices provided the structure is dominated by a single mode of vibration. The same method was used to optimally design supplemental dampers for a seven story structure [10].

The objective of this research venture is to adapt the design of supplemental PFVD for buildings to truss towers. One of the challenges for a truss tower is that the levels at which the masses are concentrated are far apart which poses some difficulties in realistically designing dampers between those specific levels only using current optimal design methods. The goal here is to develop a method for applying the optimal design of dampers to truss towers while including intermediate levels where the masses are not concentrated. This can be done by converting a 3D truss tower model to its dynamically equivalent 2D lumped mass model using the bi-model method [16]. From the 2D lumped mass model the optimal gain matrix is calculated on LQR algorithm [15]. The optimal gain matrix is then transformed to its equivalent form for the corresponding 3D truss tower model. Once the gain matrix is in the form consistent with the 3D model, the single mode estimator approach is used to calculate the optimal damping coefficients for the truss tower. To evaluate the effectiveness of this method, the response of the truss tower

with and without the optimally designed supplemental PFVD's is analyzed for seismic loads using the bi-model method. The subsequent sections provide a detailed description of the theory behind this method, the computational methodology developed for its implementation, and finally a numerical example along with results to establish the validity and efficiency of the proposed method.

## 2.0 THEORY

### 2.1 Bi-model Method

For the dynamic analysis of large truss towers the 3D finite element model can prove to be very time consuming and hence analyzing an equivalent 2D lumped mass model is common [16]. Additionally the technique presented in [15] for calculating the supplemental PFVD was developed for a 2D lumped mass model. The bi-model method serves as an excellent way to calculate the damping coefficient and to analyze a 3D model. The following assumptions were made in order for the equivalent 2D lumped mass model to dynamically represent the 3D finite element model for analysis:

1. The entire mass of the structure along with components is concentrated at specific levels of the 3D model.
2. The average motion (displacement, velocity, acceleration) of the nodes at each of these levels of the 3D model is the motion of the entire level.
3. At any given time only the horizontal motion in one direction due to a dynamic load is considered.

By making the above assumptions, the *n*DOF 3D model can be represented by a dynamically equivalent *N*DOF 2D lumped mass model.

### 2.2 Governing Equation of Motion

The equation of motion can be written as

$$\mathbf{M}\ddot{\mathbf{X}}(t) + \mathbf{C}\dot{\mathbf{X}}(t) + \mathbf{K}\mathbf{X}(t) = \mathbf{D}\mathbf{u}(t) - \mathbf{M}\mathbf{1}\ddot{X}_g(t), \quad (1)$$

where **M**, **C** and **K** are the $N \times N$ sized mass, damping and stiffness matrices, respectively. The mass matrix is a diagonal matrix with the diagonal elements constituting of the mass concentrated at the corresponding level. $\ddot{\mathbf{X}}(t), \dot{\mathbf{X}}(t)$ and $\mathbf{X}(t)$ are the $N \times 1$ sized relative to ground acceleration, velocity and displacement vectors, respectively. **D** is the $N \times m$ matrix indicating the location or point of application of the $m \times 1$ control force vector $\mathbf{u}(t)$, where $m$ is

the number of control devices. $\ddot{X}_g(t)$ represents the ground acceleration for an earthquake and **1** is a $N \times 1$ unit vector.

The equation of motion can also be written in the following state-space formulation

$$\dot{\mathbf{z}}(t) = \mathbf{A}\mathbf{z}(t) + \mathbf{B}\mathbf{u}(t) + \mathbf{H}\ddot{X}_g(t), \tag{2}$$

where

$\mathbf{z}(t) = \begin{bmatrix} \mathbf{X}(t) \\ \dot{\mathbf{X}}(t) \end{bmatrix}$ (states of the system, $2N \times 1$),

$\mathbf{A} = \begin{bmatrix} \mathbf{0} & \mathbf{I} \\ -\mathbf{M}^{-1}\mathbf{K} & -\mathbf{M}^{-1}\mathbf{C} \end{bmatrix}$ (system matrix, $2N \times 2N$),

$\mathbf{B} = \begin{bmatrix} \mathbf{0} \\ \mathbf{M}^{-1}\mathbf{D} \end{bmatrix}$ (input location matrix for the control forces, $2N \times m$),

$\mathbf{H} = \begin{bmatrix} \mathbf{0} \\ \mathbf{M}^{-1}\mathbf{M1} \end{bmatrix}$ (input location matrix, $2N \times 1$, for the earthquake forces).

As discussed previously, the bi-model method is used as a technique to go between the 3D model and its dynamically equivalent 2D lumped mass model. Based on the assumptions stated for this method, the 2D lumped mass model's stiffness matrix **K** in equation (1) is calculated by the force method [16, 17], which is done by performing the following steps:

1. A unit force was equally divided between the nodes at the $i^{th}$ level of the 3D model where the masses are concentrated and applied at each of those nodes, one level at a time.
2. The average horizontal displacements of the nodes at any other level where the masses are concentrated, $j$, due to the load applied at the $i^{\text{th}}$ level was computed as the flexibility coefficient $\delta_{ji}$ ($i, j$=1,2…$N$)
3. The resulting $N \times N$ flexibility matrix was inverted to obtain the 2D lumped mass stiffness matrix **K**.

### 2.3 Optimal Design of Dampers for Buildings

The authors of [15] present various techniques to calculate the optimal damping coefficient for supplemental dampers based on active control for buildings subjected to dynamic loads. In this research venture, the "Single Mode Approach" has been adopted for a truss tower with passive control devices for the damping.

Using the LQR algorithm [19], the control force $\mathbf{u}(t)$ is obtained by minimizing the performance index $J$ over the duration of the excitation, say $t_f$:

$$J = \int_0^{t_f} (\mathbf{z}^T(t)\mathbf{Q}\mathbf{z}(t) + \mathbf{u}^T(t)\mathbf{R}\mathbf{u}(t))dt\,, \tag{3}$$

where $\mathbf{R}$ ($m \times m$) and $\mathbf{Q}$ ($2N \times 2N$) are the weighting matrices for the factors of the optimization. The variations of the two weighting matrices affect the optimization of the technique. Varying $\mathbf{Q}$ affects the states (displacement and velocity) while that of $\mathbf{R}$ affects the control forces. This will be discussed in detail in section 4.0.

As presented in [15], for the sake of simplicity, the control force in equation (3) is assumed to be of linear form and can hence be expressed as:

$$\mathbf{u}(t) = \mathbf{G}\mathbf{z}(t) \tag{4a}$$

or

$$\mathbf{u}(t) = \mathbf{G}_x\mathbf{X}(t) + \mathbf{G}_{\dot{x}}\dot{\mathbf{X}}(t)\,, \tag{4b}$$

where $\mathbf{G}$ ($m \times 2N$) is the gain matrix that contains the constant coefficients for the control devices. The gain matrix is obtained from the solution of the following equation

$$\mathbf{G} = -\tfrac{1}{2}\mathbf{R}^{-1}\mathbf{B}^{\mathbf{T}}\mathbf{P}, \tag{5}$$

where $\mathbf{P}$ is the solution of the Algebraic Ricatti Equation (ARE):

$$\mathbf{P}\mathbf{A} + \mathbf{A}^T\mathbf{P} - \frac{1}{2}\mathbf{P}\mathbf{B}\mathbf{R}^{-1}\mathbf{B}^T\mathbf{P} + 2\mathbf{Q} = 0\,. \tag{6}$$

In adopting active control theory for the optimal design of PFVD only the velocity gains are considered as the force from a PFVD is a function of the velocity between the locations of the dampers on a structure. The velocity gains can also be obtained in their drift format by performing the following action on the velocity gain matrix:

$$\mathbf{G}_{\dot{d}} = \mathbf{T}_N^T \mathbf{G}_{\dot{x}} \mathbf{T}_N , \tag{7}$$

where $T_N$ is the transformation matrix which is a lower-diagonal unity matrix of size $N \times N$.

As per the single mode approach described in [15], the damping coefficients (to eventually obtain the control forces to be applied to the structure due to the presence of the passive dampers) are obtained from the formula:

$$\Delta C_{d_k} = \frac{\sum_j G_{\dot{d}_{kj}} \Phi_{d_{ji}}}{\Phi_{d_{ki}}}, \tag{8}$$

where $\mathbf{G}_{\dot{d}}$ represents the velocity gain matrix in drift form and $\mathbf{\Phi}_d$ represents the normalized drift mode shapes, $k = 1,2..m$. The optimal damping coefficients in equation (8) are tailored for a building structure where the masses are concentrated at levels relatively close to one another.

### 2.4 Optimal Design of Dampers for Truss Towers

As mentioned in 2.3, the above described method for calculating the optimal damping coefficients was developed for 2D lumped mass model for buildings and adopting that for a truss tower is the goal here. One of the challenges for a truss tower is that the levels at which the masses are concentrated are far apart which poses some difficulties in realistically designing dampers between those specific levels only. The objective of this research venture is to develop a method for applying the optimal design of dampers for buildings to truss towers while including intermediate levels where the masses are not concentrated.

In adapting the single mode approach for truss towers, equation (8) can be rewritten as:

$$\Delta c_{d_k} = \frac{\sum_j g_{\dot{d}_{kj}} \phi_{d_{ji}}}{\phi_{d_{ki}}}, \tag{9}$$

where

$$\mathbf{g}_{\dot{d}} = \mathbf{T}_n^T \mathbf{g}_{\dot{x}} \mathbf{T}_n , \tag{10}$$

and

(11)

$\boldsymbol{\phi}_d = \mathbf{T}_n^{-1}\boldsymbol{\phi}$,

where (12)

$\mathbf{g}_{\dot{x}} = \mathbf{S}\mathbf{G}_{\dot{x}}\mathbf{K}^{-1}$,

and (13)

$\boldsymbol{\phi} = \mathbf{V}\boldsymbol{\Phi}$.

In equation (9), $i$ and $j$ are redefined to be $i, j = 1,2..n$, and $k = 1,2..l$, where $l$ is the number of control devices on the $n$DOF 3D truss model. In equations (10)-(13), $\mathbf{T}_n$ is a $n \times n$ lower diagonal unity matrix, and **S** and **V** are matrices for the transformation between the $N$DOF and $n$DOF models. The matrices **S** and **V** are expressed as:

$\mathbf{S} = \mathbf{f}^{-1}\mathbf{J}$ (14)

and

$\mathbf{V} = \mathbf{E}\mathbf{K}$, (15)

where **f** and **E** are flexibility matrices determined using the force method on the 3D truss tower model as follows: (1) **f** is the $n \times n$ flexibility matrix for the case with the loads applied at all levels of the $n$DOF system and deflections for all $n$ levels and (2) **E** is the $n \times N$ flexibility matrix for the case with loads applied at the main levels and deflections computed for all levels.

Upon calculating the damping coefficients in Equation (9), the control force exerted on the tower from a passive damper with a chevron braced configuration is obtained simply by multiplying the damping coefficient by the corresponding relative velocity between the points where the damper is connected, and is given as:

$\mathbf{f}_{cd}(t) = \Delta\mathbf{c}_d\,\dot{\mathbf{x}}_d(t)$, (16)

where $\Delta\mathbf{c}_d$ is the $n$ x $n$ diagonal matrix containing the damping coefficients calculated from equation (9), and $\dot{\mathbf{x}}_d(t)$ is a $n$ x 1 vector of relative velocities between the points where the dampers are connected on the 3D truss tower, and are expressed as:

$\dot{\mathbf{x}}_d(t) = \mathbf{T}_n^{-1}\dot{\mathbf{x}}(t)$, (17)

where

(18)

$\dot{\mathbf{x}}(t) = \mathbf{V}\dot{\mathbf{X}}(t)$ .

The control force calculated in equation (16) is converted to its relative to ground form by:

$$\mathbf{f}_c(t) = (\mathbf{T}n^T)^{-1}\mathbf{f}_{cd}(t). \quad (19)$$

This relative to ground force is then converted to its equivalent *N*DOF form and in order to transform the control forces in equation (19) to a form consistent with equation (1), the following transformation is necessary:

$$\mathbf{F}_c(t) = \mathbf{L}\mathbf{f}_c(t), \quad (20)$$

where

$\mathbf{L} = \mathbf{K}\mathbf{W}$ and $\mathbf{W}$ is the $N \times n$ flexibility matrix for the case with loads applied at all levels and deflections computed for the main levels.

Calculating the control force as shown in equation (20), and using this value for $\mathbf{u}(t)$ in equation (1) (i.e. $\mathbf{u}(t) = \mathbf{F}_c(t)$), the *n*DOF 3D model can be analyzed for optimal design of dampers using the *N*DOF dynamically equivalent 2D lumped mass model. The computational methodology for the above explained method is outlined in the next section.

## 3.0 COMPUTATIONAL METHODOLOGY

The computational methodology for design of optimal dampers, and subsequent dynamic analysis, was executed by developing a MATLAB simulation model. The codes are included in Appendix A. The stiffness matrix for the 3D model is calculated using direct stiffness method [5]. The stiffness matrix of the dynamically equivalent 2D lumped mass model is then computed through the force method as described in the previous section. Similarly, the transformation matrices as outlined in section 2.4 are computed. Once the various characteristic matrices of the structure such as the mass, stiffness, and damping matrices are calculated, the transformation matrices are computed, and the optimal damping coefficients of the supplemental dampers are determined, codes are set up to simulate the response of the structure to seismic loads. The simulation is executed to procure the uncontrolled case, i.e. the response of the structure without any supplemental dampers. This uncontrolled response is stored and the simulation is once again executed for the controlled case, i.e. the response of the structure with supplemental dampers.

### 3.1 Optimal Design

To calculate the optimal damping coefficients for supplemental dampers prior to the dynamic analysis of the 3D truss model, the following steps are performed:

1. Calculate the relative to ground gain matrix $\mathbf{G}$ for the *N*DOF system (equation 5).

2. Transform the relative to ground velocity gains $\mathbf{G}_{\dot{x}}$ for the *N*DOF system to the relative to ground velocity gains $\mathbf{g}_{\dot{x}}$ for the *n*DOF system (equation 12).

3. Transform the relative to ground velocity gains $\mathbf{g}_{\dot{x}}$ for the *n*DOF system to drift form $\mathbf{g}_{\dot{d}}$ (equation 10).

4. Calculate the relative to ground mode shapes $\mathbf{\Phi}$ for the *N*DOF system.

5. Transform the relative to ground mode shapes $\mathbf{\Phi}$ for the *N*DOF system to the relative to ground mode shapes $\boldsymbol{\phi}$ for the *n*DOF system (equation 13).

6. Transform the relative to ground *n*DOF mode shapes $\boldsymbol{\phi}$ to drift form $\boldsymbol{\phi}_d$ (equation 11).

7. Calculate the optimal damping coefficients for the *n*DOF system using the quantities computed in steps 3 and 6 (equation 9).

The following flowchart illustrates the above steps:

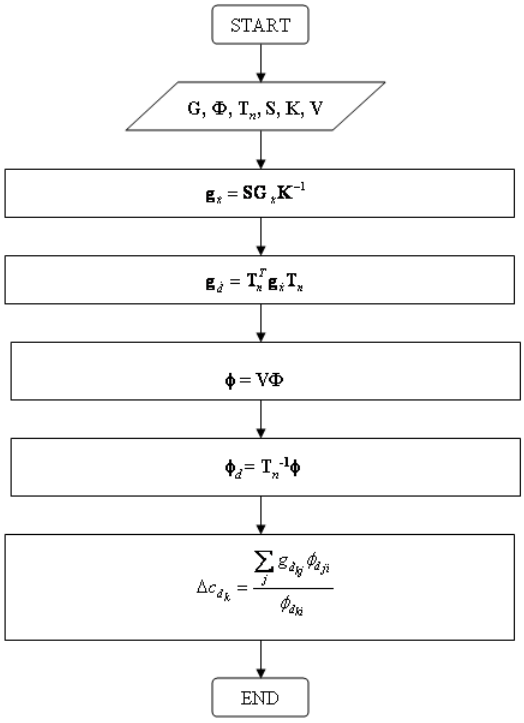


Figure 1: Optimal Damping Design Flowchart

### 3.2 Dynamic Analysis (Bi-model Method)

Once the optimal damping coefficients are calculated as outlined above, the response of the 3D truss tower is determined through the bi-model method by performing the following steps:

1. Calculate the response (displacement, velocity and acceleration) of the 2D *N*DOF lumped mass model for the first time step.

2. Transform the relative to ground velocity $\dot{\mathbf{X}}(t)$ of the NDOF system to the relative to ground velocity $\dot{\mathbf{x}}(t)$ for the *n*DOF system (equation 18).

3. Transform the relative to ground velocity $\dot{\mathbf{x}}(t)$ for the *n*DOF system to drift form $\dot{\mathbf{x}}_d(t)$ (equation 17).

4. Calculate the control force in its drift form based on the optimal design of damping coefficient for a damper arranged in a chevron braced configuration for the *n*DOF system (equation 16).

5. Transform the control force in its drift form to the relative to ground force for the *n*DOF system (equation 19).

6. Transform the relative to ground control force for the *n*DOF system to the relative to ground force for the *N*DOF system (Equation 20).

7. Calculate the response of the structure for the control force calculated in step 6 for the next time step.

8. Repeat steps 1 through 7 for all time steps.

The following flowchart illustrates the above steps:

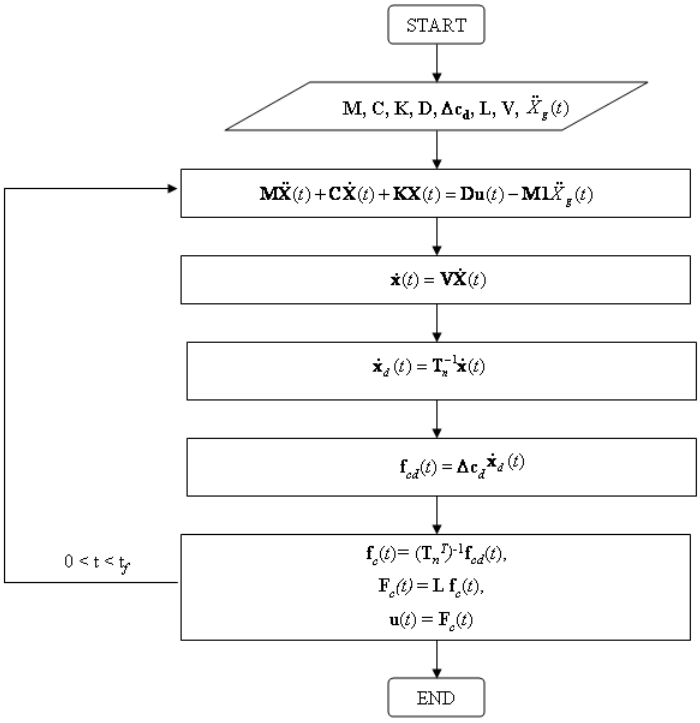


Figure 2: Dynamic Analysis Flowchart

A numerical example is presented in the next section to demonstrate the above and the corresponding results are presented.

## 4.0 NUMERICAL EXAMPLE

As explained in section 2.0, the goal of this research is to adapt an optimal technique to design dampers developed for buildings to truss towers. In doing so the method will allow for design of dampers for levels of the truss tower where masses are not concentrated. To do so, the computational methodology presented in section 3.0 was implemented on a truss tower model. Four variations of the optimal design approach were tested on the truss model to determine the most efficient method. This method was then validated by comparing with a performance based design approach. Upon validation additional simulations were conducted to demonstrate the efficiency of this optimal design method in reducing the response of the truss model subjected to seismic loads of varying intensity. For this purpose, twenty four earthquake data were used to compute the tower's uncontrolled and controlled response.

### 4.1 Tower Model

The truss tower model used is similar to the model used by the authors of [16] and is shown in Figure 3 below. From the 3D truss tower model shown in Figure 3(a), the masses are taken to be concentrated at every 8m for the equivalent 2D lumped mass model shown in Figure 3(b). The plan view shown on Figure 3(c) corresponds to these three levels. The sectional areas of the vertical members are $3.7953 \times 10^{-3}$ m$^2$, the horizontal members are $1.3193 \times 10^{-3}$ m$^2$ and that of the diagonal members, including the ones on the plan view as shown on Figure 3(c), are $3.1903 \times 10^{-4}$ m$^2$. The modulus of elasticity of the material of the truss members is $2.06 \times 10^{11}$ Pa.

The mass at each main level was taken to be $2 \times 10^5$ kg and the corresponding diagonal mass matrix **M** is given by:

$$\mathbf{M} = \begin{bmatrix} 2 & 0 & 0 \\ 0 & 2 & 0 \\ 0 & 0 & 2 \end{bmatrix} \times 10^5 \text{ kg.}$$

A MATLAB code was developed to obtain the stiffness matrix (132 x 132) for this structure using direct stiffness method [18]. The 2D lumped mass stiffness matrix **K** for this model, as outlined in section 2.0, was calculated to be:

$$\mathbf{K} = \begin{bmatrix} 1.07 & -0.56 & 0.056 \\ -0.56 & 1.05 & -0.49 \\ 0.06 & -0.49 & 0.42 \end{bmatrix} \times 10^7 \text{ N/m.}$$

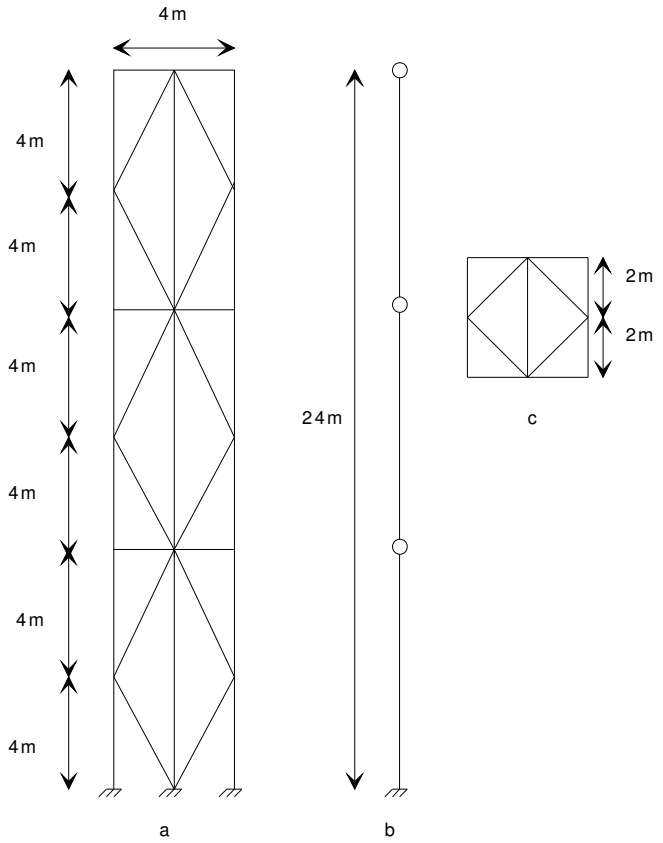


Figure3. (a) Side View of Truss Model (b) 2D Lumped Mass Model (c) Plan View

The authors of [16] assumed Rayleigh damping for the model and observed that the structural damping ratio was 1.5% for all modes of vibration. Hence a uniform modal damping of 1.5% was adopted to calculate the damping matrix **C** as:

$$\mathbf{C} = \begin{bmatrix} 4.19 & -1.27 & -0.13 \\ -1.27 & 3.89 & -1.47 \\ -0.13 & -1.47 & 2.30 \end{bmatrix} \times 10^4 \text{ N-sec/m.}$$

To validate the above model the natural vibration periods for the truss model was calculated and compared with the same presented by the authors of [16]. A Comparison of columns (2) – (4) shows a good agreement between the two models.

Table 1: Natural Vibration Periods

| **Model** **(1)** | **First (sec)** **(2)** | **Second (sec)** **(3)** | **Third (sec)** **(4)** |
|---|---|---|---|
| Qu et. al. | 3.12 | 1.05 | 0.67 |
| Current Model | 3.12 | 1.05 | 0.67 |

**4.2 Optimal Design**

Using the optimal design for calculating damping coefficients for the truss model, a total of twenty four earthquake data were used. Table 2 lists the earthquakes used in the simulation. The simulation is executed to procure the uncontrolled response, i.e. the response of the structure without any supplemental dampers. This uncontrolled response is stored and the simulation is once again executed for the controlled case, i.e. the response of the structure with the optimally designed supplemental dampers. The effect of the dampers on controlling the response of the structure was evaluated by calculating the mean response ratios (RR), which is the ratio of the controlled to the uncontrolled response of the structure for a given level averaged of the twenty four earthquakes.

Table 2: Earthquake Data [19]

| **Earthquake (1)** | **Magnitude (Richter) (2)** | **Peak Acceleration (g) (3)** |
|---|---|---|
| Kobe, Japan | 7.2 | 0.83 |
| Hachinohe, Japan | 6.8 | 0.23 |
| El Centro, California | 7.1 | 0.35 |
| Northridge, California | 6.7 | 0.84 |
| Northridge 90°, California | | 0.34 |
| Northridge 360°, California | | 0.31 |
| Northridge 265°, California | | 0.43 |
| Northridge 175°, California | | 0.41 |
| Ferndale S44W, Northwestern California | 5.8 | 0.10 |
| Ferndale N46W, Northwestern California | | 0.11 |
| San Francisco N10E, California | 5.3 | 0.08 |
| San Francisco S80E, California | | 0.10 |
| Helena S00W, Montana | 6.0 | 0.15 |
| Helena S90W, Montana | | 0.14 |
| Parkfield N65W, California | 5.6 | 0.27 |
| Parkfield S25W, California | | 0.35 |
| San Fernando S16E, California | 6.4 | 1.17 |
| San Fernando S74W, California | | 1.07 |
| San Fernando N36E, California | | 0.09 |
| San Fernando N54W, California | | 0.12 |
| Loma Prieta, Corralitos 90°, California | 7.1 | 0.48 |
| Loma Prieta, Corralitos 0°, California | | 0.63 |
| Loma Prieta, Capitola 90°, California | | 0.39 |
| Loma Prieta, Capitola 0°, California | | 0.47 |

For the controlled case the optimal damping coefficients for the supplemental dampers were calculated as per equation (9) for the first mode using four variations of the optimal design method. This is achieved by varying the weighting matrices **Q** and **R** in the LQR algorithm. The sizing and elements of **Q** affect the states (displacement and velocity) of the structure. The sizing and elements of **R** affect the control force acting on the structure. The four variations on the optimization can be summarized as follows:

1. Equal weights:

$$\mathbf{R} = 10^{-p}\mathbf{I}_{3\times3};\ \mathbf{Q} = \mathbf{I}_{6\times6}, \tag{21}$$

**Q**, in this case, applies the weights equally towards the structure's responses.

2. Velocity control:

$$\mathbf{R} = 10^{-p}\mathbf{I}_{3\times3};\ \mathbf{Q} = \begin{bmatrix} \mathbf{0} & \mathbf{0} \\ \mathbf{0} & \mathbf{I}_{3\times3} \end{bmatrix} \tag{22}$$

**Q**, in this case, applies the weights towards the structure's velocity only.

3. Displacement control:

$$\mathbf{R} = 10^{-p}\mathbf{I}_{3\times3};\ \mathbf{Q} = \begin{bmatrix} \mathbf{I}_{3\times3} & \mathbf{0} \\ \mathbf{0} & \mathbf{0} \end{bmatrix} \tag{23}$$

**Q**, in this case, applies the weights equally towards the structure's displacement only.

4. Energy Minimization:

$$\mathbf{R} = \mathbf{K}^{-1};\ \mathbf{Q} = \begin{bmatrix} \mathbf{K} & \mathbf{0} \\ \mathbf{0} & \mathbf{M} \end{bmatrix} 10^{-p} \tag{24}$$

The weighting matrices used for this approach are as described in [19].

Each of the above four approach's effect were simulated on the twenty four earthquakes. To simplify this process, the uncontrolled response of the building averaged over the earthquakes was computed and it was observed that the second level of the 3D model had the largest absolute acceleration. Hence, the response of this level was chosen to study the effectiveness of the above described methods.

To determine the optimal design of the supplemental dampers, the simulation was executed for a series of values of *p*. To identify the value of *p* that gives the best response for each of the above mentioned approaches, graphs were plotted between the absolute acceleration RR and inter-story drift RR of the second level of the truss model versus *p*. The RR is the ratio of the controlled response to that of the uncontrolled response. The value of *p* for which the two curves intersect

was taken to be the optimal value. The following four graphs were plotted for the four optimal design approaches:

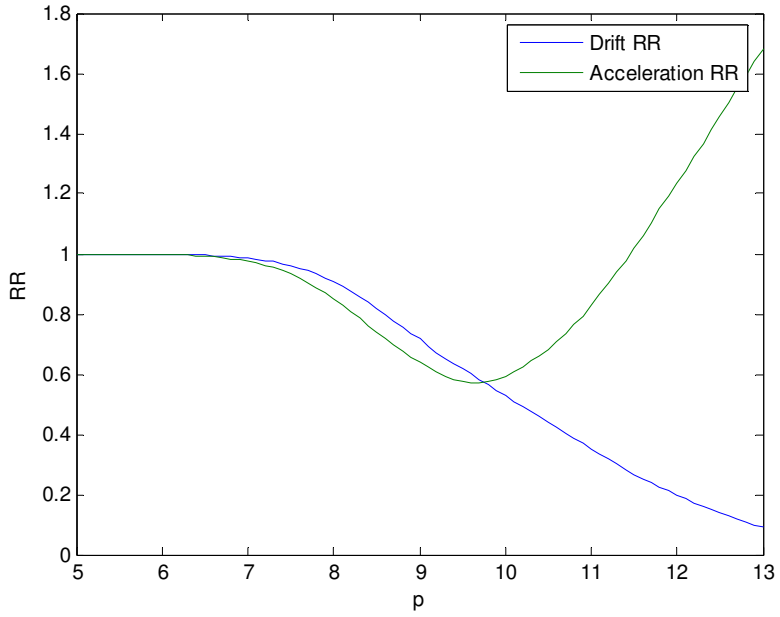


Figure 4: Equal Weights, $p$=9.75

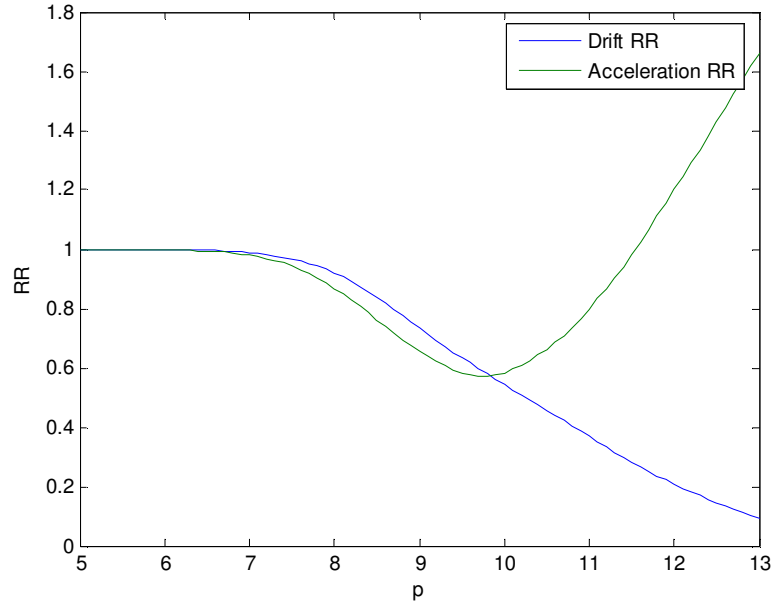


Figure 5: Velocity Control, $p$=9.85

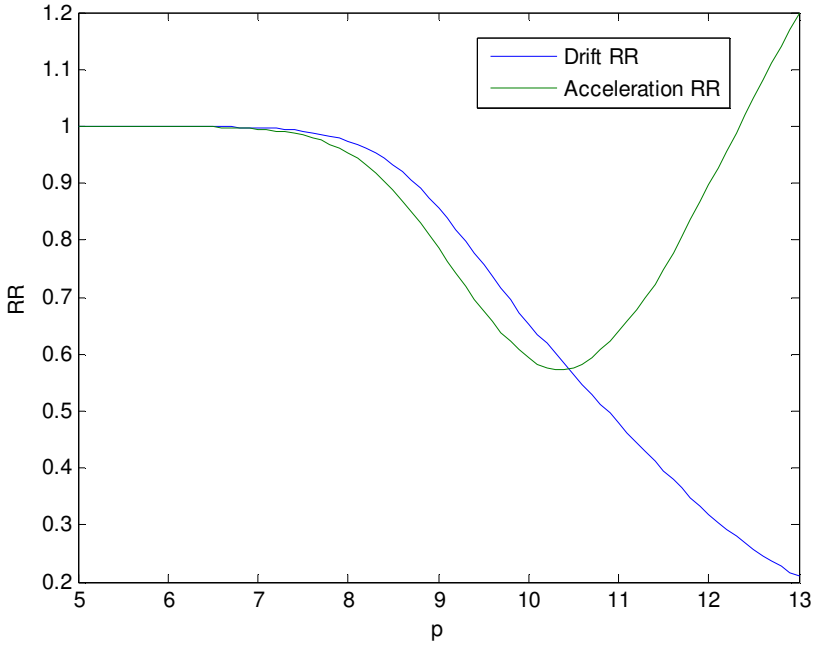


Figure 6: Displacement Control, $p$=10.5

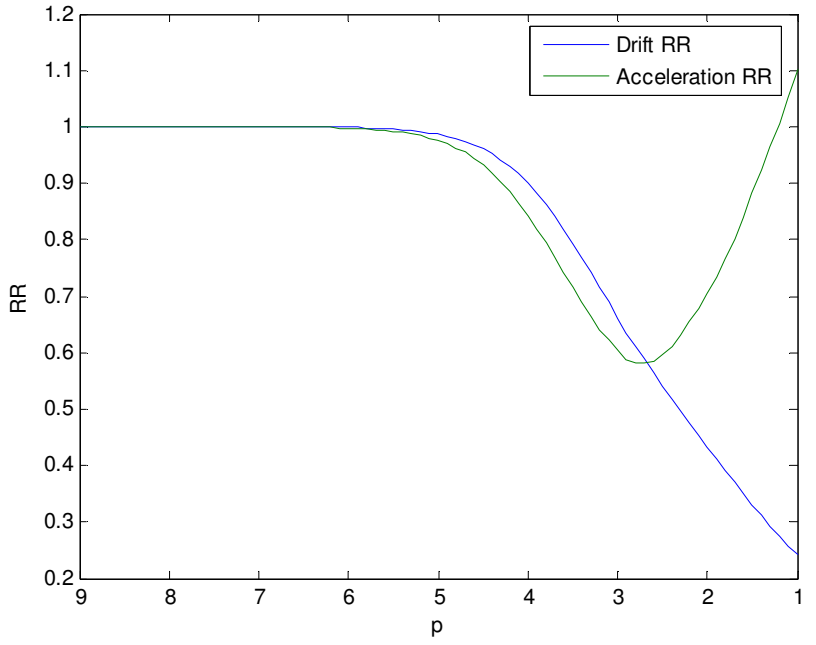


Figure 7: Energy Minimization, $p$=2.65

It can be observed that clearly the lower the RR the better the optimization. But the control force $\mathbf{f}_c(t)$ that is required for the response control at each level of the 6DOF system also plays a role in determining the best technique. For this purpose, the simulation is once again executed for each of the above four approaches for only the corresponding $p$ value. The following tables summarize the results for each case:

Table 3: Equal Weights $p$=9.75

| **Level**<br>**(1)** | **Δc drift**<br>**$10^5$ N-sec/m**<br>**(2)** | **Drift RR**<br>**(3)** | **Acceleration RR**<br>**(4)** | **Control Force**<br>**$10^5$ N**<br>**(5)** |
|---|---|---|---|---|
| 1 | 8.61 | 0.57 | 0.57 | 1.41 |
| 2 | 8.59 | 0.57 | 0.57 | 1.42 |
| 3 | 6.83 | 0.59 | 0.54 | 0.75 |
| 4 | 6.77 | 0.60 | 0.41 | 0.74 |
| 5 | 5.08 | 0.49 | 0.62 | 0.64 |
| 6 | 4.99 | 0.49 | 0.46 | 0.63 |

Table 4: Velocity Control $p$=9.85

| **Level**<br>**(1)** | **Δc drift**<br>**$10^5$ N-sec/m**<br>**(2)** | **Drift RR**<br>**(3)** | **Acceleration RR**<br>**(4)** | **Control Force**<br>**$10^5$ N**<br>**(5)** |
|---|---|---|---|---|
| 1 | 8.66 | 0.57 | 0.57 | 1.42 |
| 2 | 8.64 | 0.57 | 0.57 | 1.42 |
| 3 | 6.87 | 0.59 | 0.54 | 0.75 |
| 4 | 6.81 | 0.60 | 0.41 | 0.74 |
| 5 | 5.11 | 0.49 | 0.62 | 0.64 |
| 6 | 5.02 | 0.49 | 0.46 | 0.63 |

Table 5: Displacement Control $p$=10.5

| **Level** **(1)** | **Δc drift $10^5$ N-sec/m (2)** | **Drift RR** **(3)** | **Acceleration RR (4)** | **Control Force $10^5$ N (5)** |
|---|---|---|---|---|
| 1 | 9.09 | 0.57 | 0.57 | 1.47 |
| 2 | 9.06 | 0.56 | 0.57 | 1.48 |
| 3 | 7.21 | 0.59 | 0.53 | 0.78 |
| 4 | 7.15 | 0.59 | 0.40 | 0.77 |
| 5 | 5.36 | 0.49 | 0.61 | 0.65 |
| 6 | 5.26 | 0.49 | 0.45 | 0.64 |

Table 6: Energy Minimization $p$=2.65

| **Level** **(1)** | **Δc drift $10^5$ N-sec/m (2)** | **Drift RR** **(3)** | **Acceleration RR (4)** | **Control Force $10^5$ N (5)** |
|---|---|---|---|---|
| 1 | 8.82 | 0.58 | 0.58 | 1.44 |
| 2 | 8.79 | 0.58 | 0.58 | 1.45 |
| 3 | 6.43 | 0.61 | 0.55 | 0.71 |
| 4 | 6.38 | 0.61 | 0.43 | 0.71 |
| 5 | 3.44 | 0.53 | 0.62 | 0.48 |
| 6 | 3.38 | 0.53 | 0.49 | 0.47 |

Upon comparing Tables 3-6, it was observed that the responses and control forces were very similar to one another. The sum total of the control force for all six levels, and the RR's of the second level were considered as the deciding parameters. The four results are presented in Table 7 below. The energy minimization approach requires the least control force for providing almost the same controlled response as the other techniques. Hence, this method is considered the best technique to optimally design the dampers.

Table 7: Comparison of Approaches

| **Method**<br><br>**(1)** | **Drift RR Second Level**<br>**(2)** | **Acceleration RR Second Level**<br>**(3)** | **Sum Total Control Force ($10^5$N)**<br>**(4)** |
|---|---|---|---|
| Equal Weights | 0.57 | 0.57 | 5.58 |
| Velocity Control | 0.57 | 0.57 | 5.60 |
| Displacement Control | 0.56 | 0.57 | 5.80 |
| Energy Minimization | 0.58 | 0.58 | 5.26 |

### 4.3 Performance Based Design

As a way to validate the optimal design technique, a performance based design simulation was executed to arrive at an average damping value without involving the structural properties to design the damper. The range of damping coefficients selected for this simulation was randomly selected till an exact value was obtained again by plotting a graph, again, between the range of damping coefficients and the RR's of the second level.

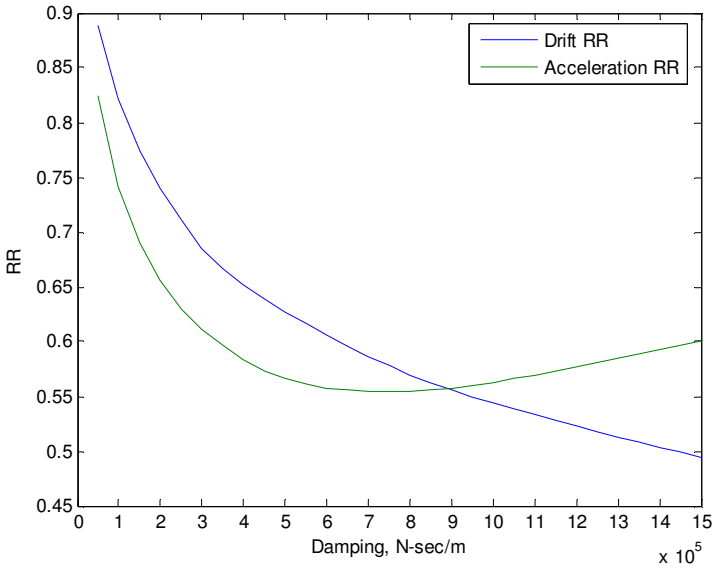


Figure 8: Performance Based Design

The exact damping value used for this design is 900000 N-sec/m, as determined from the intersection point on Figure 8 above. The simulation was executed for this single value and the following responses were calculated:

Table 8: Performance Based Design

| **Level**<br>**(1)** | **Δc drift**<br>**$10^5$ N-sec/m**<br>**(2)** | **Drift RR**<br>**(3)** | **Acceleration RR**<br>**(4)** | **Control Force**<br>**$10^4$ N**<br>**(5)** |
|---|---|---|---|---|
| 1 | 9.00 | 0.56 | 0.56 | 1.46 |
| 2 | 9.00 | 0.55 | 0.56 | 1.47 |
| 3 | 9.00 | 0.56 | 0.51 | 0.94 |
| 4 | 9.00 | 0.56 | 0.37 | 0.94 |
| 5 | 9.00 | 0.43 | 0.60 | 0.89 |
| 6 | 9.00 | 0.43 | 0.40 | 0.89 |

Once again, comparing this to the output of the energy minimization method, it can be summarized as shown below in Table 9. The comparison serves as a way to validate the optimal design approach. It can be observed that for a 5% reduction in drift RR and a 3% reduction in acceleration RR, the performance based design requires a 20% increase in control forces. Once again, it can be concluded that for similar control of the response of the structure, the energy minimization method requires lesser control force and hence the best technique for the optimal design of the supplemental dampers.

Table 9: Comparison of Energy Minimization (EM) and Performance based design

| **Method**<br>**(1)** | **Drift RR**<br>**Second Level**<br>**(2)** | **Acceleration RR**<br>**Second Level**<br>**(3)** | **Sum Total Control Force ($10^5$N)**<br>**(4)** |
|---|---|---|---|
| Energy Minimization | 0.58 | 0.58 | 5.26 |
| Performance Based | 0.55 | 0.56 | 6.60 |

### 4.4 Evaluation of Optimal Design – Energy Minimization

To further investigate the effectiveness of the energy minimization, the method was tested on one large earthquake, one mid-intensity earthquake and one small earthquake. For this purpose, the large earthquake data used was Kobe, the mid-intensity earthquake data used was San Fernando N54W earthquake and the small earthquake data used was San Francisco N10E earthquake listed on the table. The uncontrolled and controlled accelerations and Interstory drifts of the structure for each of the four earthquakes were simulated and that of the second floor was plotted to obtain the following results:

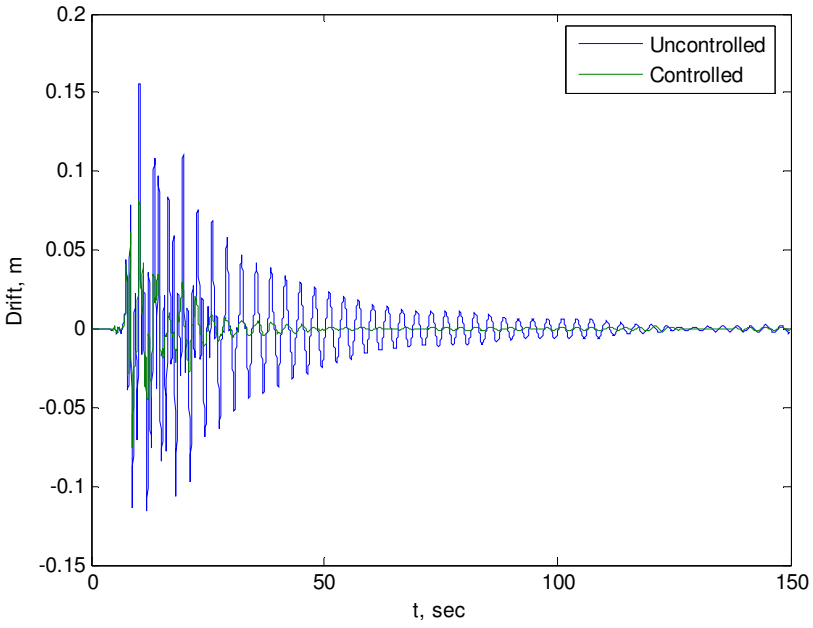


Figure 9: Kobe, Drift

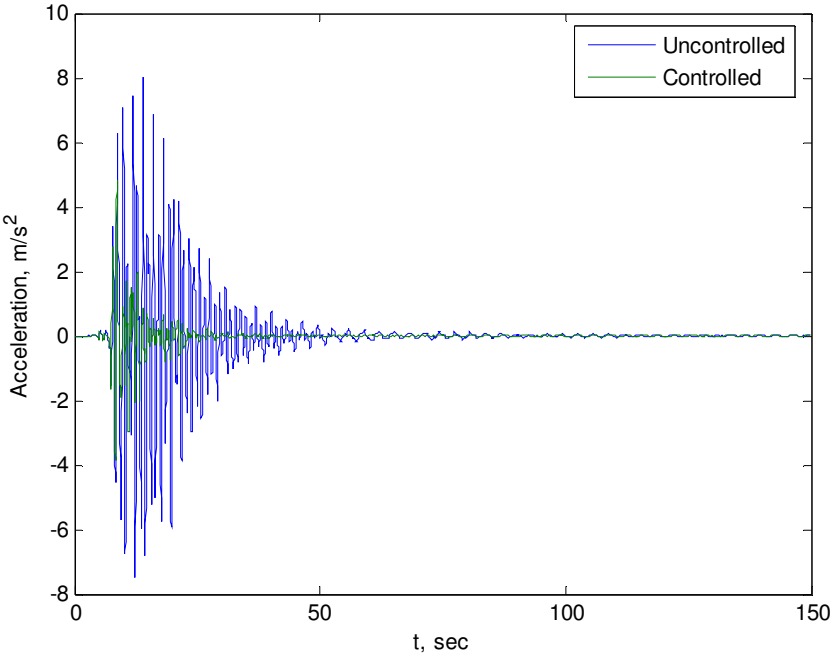


Figure 10: Kobe, Acceleration

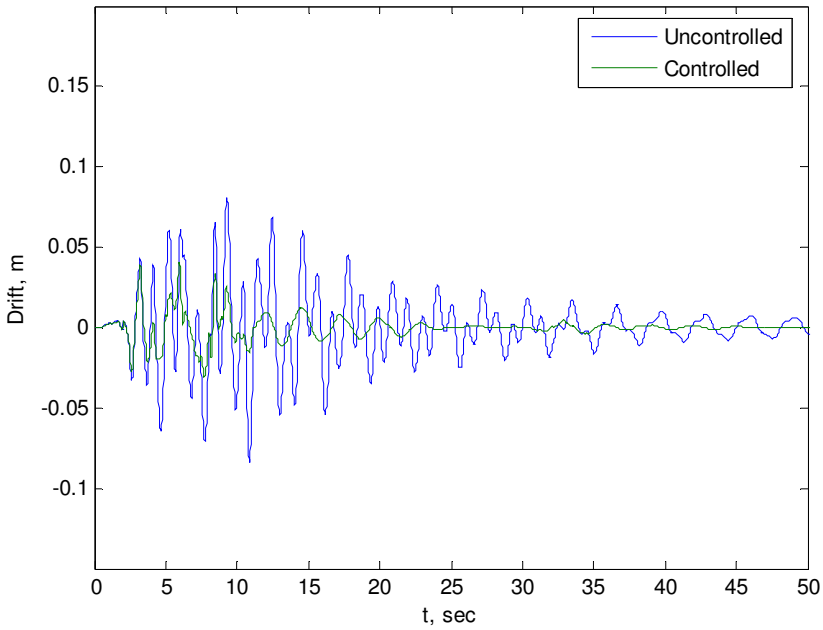


Figure 11: San Fernando, Drift

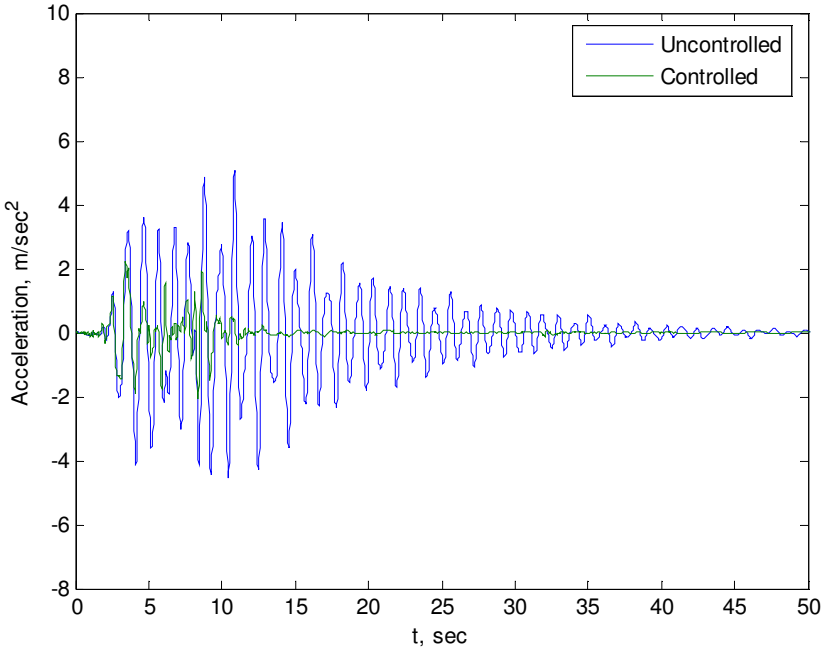


Figure 12: San Fernando, Acceleration

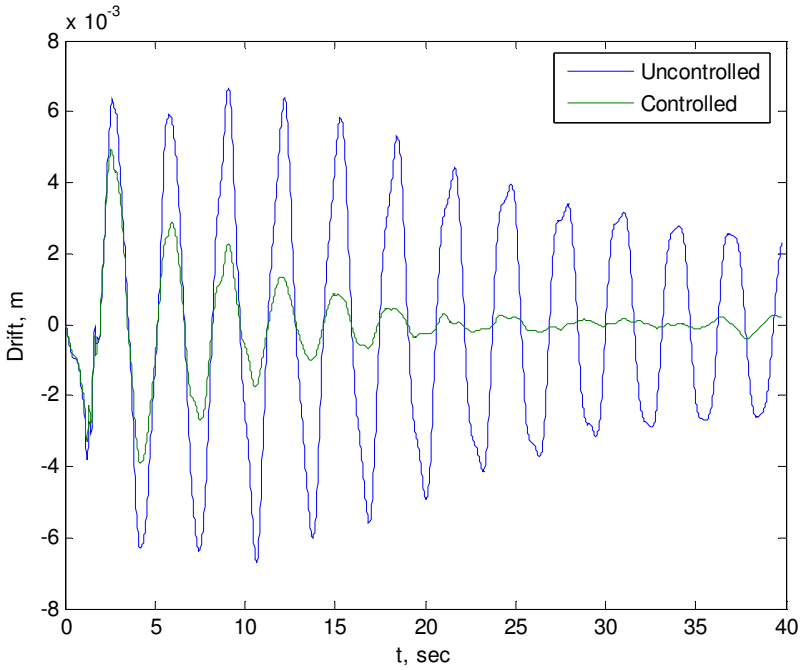


Figure 13: San Francisco, Drift

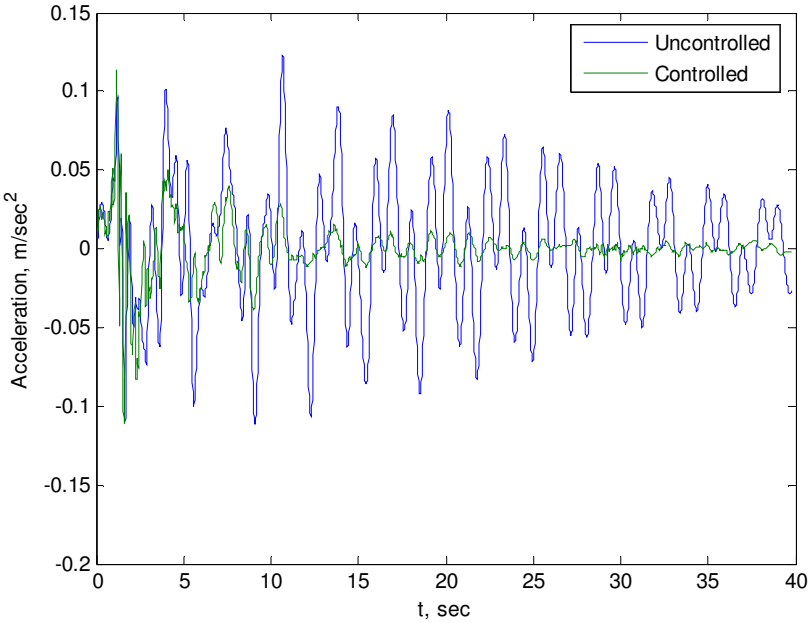


Figure 14: San Francisco, Acceleration

Below are the tables that compare the drift and acceleration RR of the three earthquakes for all six levels of the structure:

Table 10: Interstory Drift RR

| **Levels (1)** | **Kobe (2)** | **San Fernando (3)** | **San Francisco (4)** |
|---|---|---|---|
| 1 | 0.47 | 0.49 | 0.74 |
| 2 | 0.47 | 0.49 | 0.74 |
| 3 | 0.59 | 0.53 | 0.79 |
| 4 | 0.60 | 0.53 | 0.78 |
| 5 | 0.46 | 0.54 | 0.80 |
| 6 | 0.46 | 0.54 | 0.80 |

Table 11: Acceleration RR

| **Levels (1)** | **Kobe (2)** | **San Fernando (3)** | **San Francisco (4)** |
|---|---|---|---|
| 1 | 0.57 | 0.44 | 0.92 |
| 2 | 0.57 | 0.44 | 0.92 |
| 3 | 0.59 | 0.44 | 0.75 |
| 4 | 0.40 | 0.26 | 0.59 |
| 5 | 0.57 | 0.56 | 0.78 |
| 6 | 0.44 | 0.53 | 0.78 |

It can be observed that the smallest earthquake has the largest RR's. This is because the control force exerted on the structure to reduce the structure's response for a small earthquake is lower than the force for a large earthquake such as Kobe. This in turn results in the response of the structure being closer in value to the uncontrolled response and hence the larger RR. The effect of the optimal design on the large and mid-intensity earthquake are significant and it can be concluded that the optimal design of dampers for a truss tower using the energy minimization technique is an efficient method for controlling excess vibrations due to seismic loads.

## 5.0 CONCLUSIONS AND FUTURE WORK

A technique for optimal design of PFVD's for truss towers was presented. The single mode estimator method for calculating the optimal damping coefficient for supplemental dampers based on active control for buildings subjected to dynamic loads was adapted to design PFVD for truss towers. The bi-model method was used to transform the 3D truss model to its dynamically equivalent 2D lumped mass model which was used to design the supplemental dampers and analyze the structure for seismic loads. A computational methodology was developed to implement this technique. Four different optimal design approaches were tested on the model and the energy minimization approach was found to be the most efficient optimal damping method. This method was validated by comparison with a performance based design method. Comparison of results for these two methods shows that the optimally designed system requires lower control forces to achieve a similar response reduction as that of the performance based design. The energy minimization method was then implemented for three particular earthquakes of varying intensities and the controlled and uncontrolled responses of the structure for each of them were compared and thus the efficiency of the method was established.

The optimal damping design shown here shows promise for real-life truss towers. This work can further be extended to an existing truss tower to better explore its efficiency. The optimal damping design can be done for other modes of the structure. This method can also be used for an optimal design for stiffeners (braces) to be developed in the place of dampers for retrofitting existing truss towers. The optimal damping design can be done for other dynamic loads such as wind loads. Some of the above mentioned future works are currently underway.

## APPENDIX

### MATLAB Codes

1. 2D lumped mass model stiffness matrix and other transformation matrices

```
 %Define Truss Properties
%Number of members
nm=123;
DOF_tot=132;
nDOF_mem=6;
%Area of members in sq.m
A=[(1.3193/1000)*ones(24,1);(3.7953/1000)*ones(28,1);(3.1903/10000)*ones(40,1)
;(1.3193/1000)*ones(15,1);(3.7953/1000)*ones(8,1);(3.1903/10000)*ones(8,1)];

%Modulus of elasticity, in Pa (N/sq.m)
E=[2.06e11*ones(nm,1)];

%Member coordinates
cm=[0,24,0,2,24,0;
    2,24,0,4,24,0;
    0,16,0,2,16,0;
    2,16,0,4,16,0;
    0,8,0,2,8,0;
    2,8,0,4,8,0;
    2,24,4,4,24,4;
    0,24,4,2,24,4;
    2,16,4,4,16,4;
    0,16,4,2,16,4;
    2,8,4,4,8,4;
    0,8,4,2,8,4;
    4,24,0,4,24,2;
    4,24,2,4,24,4;
    4,16,0,4,16,2;
    4,16,2,4,16,4;
    4,8,0,4,8,2;
    4,8,2,4,8,4;
    0,24,2,0,24,4;
    0,24,0,0,24,2;
    0,16,2,0,16,4;
    0,16,0,0,16,2;
    0,8,2,0,8,4;
    0,8,0,0,8,2;
    2,16,0,2,24,0;
    2,8,0,2,16,0;
    2,16,4,2,24,4;
    2,8,4,2,16,4;
    4,16,2,4,24,2;
    4,8,2,4,16,2;
    0,16,2,0,24,2;
    0,8,2,0,16,2;
    0,20,0,0,24,0;
    0,16,0,0,20,0;
```

```
0,12,0,0,16,0;
0,8,0,0,12,0;
0,4,0,0,8,0;
4,20,0,4,24,0;
4,16,0,4,20,0;
4,12,0,4,16,0;
4,8,0,4,12,0;
4,4,0,4,8,0;
4,20,4,4,24,4;
4,16,4,4,20,4;
4,12,4,4,16,4;
4,8,4,4,12,4;
4,4,4,4,8,4;
0,20,4,0,24,4;
0,16,4,0,20,4;
0,12,4,0,16,4;
0,8,4,0,12,4;
0,4,4,0,8,4;
0,20,0,2,24,0;
0,12,0,2,16,0;
0,4,0,2,8,0;
2,16,0,4,20,0;
2,8,0,4,12,0;
4,20,4,2,24,4;
4,12,4,2,16,4;
4,4,4,2,8,4;
2,16,4,0,20,4;
2,8,4,0,12,4;
4,20,0,4,24,2;
4,12,0,4,16,2;
4,4,0,4,8,2;
4,16,2,4,20,4;
4,8,2,4,12,4;
0,20,4,0,24,2;
0,12,4,0,16,2;
0,4,4,0,8,2;
0,16,2,0,20,0;
0,8,2,0,12,0;
4,20,0,2,24,0;
4,12,0,2,16,0;
4,4,0,2,8,0;
2,16,0,0,20,0;
2,8,0,0,12,0;
0,20,4,2,24,4;
0,12,4,2,16,4;
0,4,4,2,8,4;
2,16,4,4,20,4;
2,8,4,4,12,4;
4,20,4,4,24,2;
4,12,4,4,16,2;
4,4,4,4,8,2;
4,16,2,4,20,0;
4,8,2,4,12,0;
0,20,0,0,24,2;
```

```
    0,12,0,0,16,2;
    0,4,0,0,8,2;
    0,16,2,0,20,4;
    0,8,2,0,12,4;
    0,24,2,2,24,4;
    2,24,0,4,24,2;
    0,16,2,2,16,4;
    2,16,0,4,16,2;
    0,8,2,2,8,4;
    2,8,0,4,8,2;
    4,24,2,2,24,4;
    2,24,0,0,24,2;
    4,16,2,2,16,4;
    2,16,0,0,16,2;
    4,8,2,2,8,4;
    2,8,0,0,8,2;
    2,24,0,2,24,4;
    2,16,0,2,16,4;
    2,8,0,2,8,4;
    2,0,0,2,8,0;
    2,0,4,2,8,4;
    4,0,2,4,8,2;
    0,0,2,0,8,2;
    0,0,0,0,4,0;
    4,0,0,4,4,0;
    4,0,4,4,4,4;
    0,0,4,0,4,4;
    2,0,0,0,4,0;
    2,0,4,4,4,4;
    4,0,2,4,4,0;
    0,0,2,0,4,4;
    0,0,2,0,4,0;
    4,0,2,4,4,4;
    2,0,4,0,4,4;
    2,0,0,4,4,0];

%Member-node vectors
%Free dof's
%Horizontal members numbering
AT(1,:)=[1,2,3,4,5,6];
AT(2,:)=[4,5,6,7,8,9];
AT(3,:)=[16,17,18,19,20,21];
AT(4,:)=[19,20,21,22,23,24];
AT(5,:)=[31,32,33,34,35,36];
AT(6,:)=[34,35,36,37,38,39];
AT(7,:)=[49,50,51,46,47,48];
AT(8,:)=[52,53,54,49,50,51];
AT(9,:)=[64,65,66,61,62,63];
AT(10,:)=[67,68,69,64,65,66];
AT(11,:)=[79,80,81,76,77,78];
AT(12,:)=[82,83,84,79,80,81];
AT(13,:)=[7,8,9,91,92,93];
AT(14,:)=[91,92,93,46,47,48];
AT(15,:)=[22,23,24,94,95,96];
```

```
AT(16,:)=[94,95,96,61,62,63];
AT(17,:)=[37,38,39,97,98,99];
AT(18,:)=[97,98,99,76,77,78];
AT(19,:)=[100,101,102,52,53,54];
AT(20,:)=[1,2,3,100,101,102];
AT(21,:)=[103,104,105,67,68,69];
AT(22,:)=[16,17,18,103,104,105];
AT(23,:)=[106,107,108,82,83,84];
AT(24,:)=[31,32,33,106,107,108];
%Tall vertical members numbering
AT(25,:)=[19,20,21,4,5,6];
AT(26,:)=[34,35,36,19,20,21];
AT(27,:)=[64,65,66,49,50,51];
AT(28,:)=[79,80,81,64,65,66];
AT(29,:)=[94,95,96,91,92,93];
AT(30,:)=[97,98,99,94,95,96];
AT(31,:)=[103,104,105,100,101,102];
AT(32,:)=[106,107,108,103,104,105];
%Short vertical members numbering
AT(33,:)=[13,14,15,1,2,3];
AT(34,:)=[16,17,18,13,14,15];
AT(35,:)=[28,29,30,16,17,18];
AT(36,:)=[31,32,33,28,29,30];
AT(37,:)=[43,44,45,31,32,33];
AT(38,:)=[10,11,12,7,8,9];
AT(39,:)=[22,23,24,10,11,12];
AT(40,:)=[25,26,27,22,23,24];
AT(41,:)=[37,38,39,25,26,27];
AT(42,:)=[40,41,42,37,38,39];
AT(43,:)=[58,59,60,46,47,48];
AT(44,:)=[61,62,63,58,59,60];
AT(45,:)=[73,74,75,61,62,63];
AT(46,:)=[76,77,78,73,74,75];
AT(47,:)=[88,89,90,76,77,78];
AT(48,:)=[55,56,57,52,53,54];
AT(49,:)=[67,68,69,55,56,57];
AT(50,:)=[70,71,72,67,68,69];
AT(51,:)=[82,83,84,70,71,72];
AT(52,:)=[85,86,87,82,83,84];
%Brace acute
AT(53,:)=[13,14,15,4,5,6];
AT(54,:)=[28,29,30,19,20,21];
AT(55,:)=[43,44,45,34,35,36];
AT(56,:)=[19,20,21,10,11,12];
AT(57,:)=[34,35,36,25,26,27];
AT(58,:)=[58,59,60,49,50,51];
AT(59,:)=[73,74,75,64,65,66];
AT(60,:)=[88,89,90,79,80,81];
AT(61,:)=[64,65,66,55,56,57];
AT(62,:)=[79,80,81,70,71,72];
AT(63,:)=[10,11,12,91,92,93];
AT(64,:)=[25,26,27,94,95,96];
AT(65,:)=[40,41,42,97,98,99];
AT(66,:)=[94,95,96,58,59,60];
```

```
AT(67,:)=[97,98,99,73,74,75];
AT(68,:)=[55,56,57,100,101,102];
AT(69,:)=[70,71,72,103,104,105];
AT(70,:)=[85,86,87,106,107,108];
AT(71,:)=[103,104,105,13,14,15];
AT(72,:)=[106,107,108,28,29,30];
%Brace obtuse
AT(73,:)=[10,11,12,4,5,6];
AT(74,:)=[25,26,27,19,20,21];
AT(75,:)=[40,41,42,34,35,36];
AT(76,:)=[19,20,21,13,14,15];
AT(77,:)=[34,35,36,28,29,30];
AT(78,:)=[55,56,57,49,50,51];
AT(79,:)=[70,71,72,64,65,66];
AT(80,:)=[85,86,87,79,80,81];
AT(81,:)=[64,65,66,58,59,60];
AT(82,:)=[79,80,81,73,74,75];
AT(83,:)=[58,59,60,91,92,93];
AT(84,:)=[73,74,75,94,95,96];
AT(85,:)=[88,89,90,97,98,99];
AT(86,:)=[94,95,96,10,11,12];
AT(87,:)=[97,98,99,25,26,27];
AT(88,:)=[13,14,15,100,101,102];
AT(89,:)=[28,29,30,103,104,105];
AT(90,:)=[43,44,45,106,107,108];
AT(91,:)=[103,104,105,55,56,57];
AT(92,:)=[106,107,108,70,71,72];
%Plan barce acute
AT(93,:)=[100,101,102,49,50,51];
AT(94,:)=[4,5,6,91,92,93];
AT(95,:)=[103,104,105,64,65,66];
AT(96,:)=[19,20,21,94,95,96];
AT(97,:)=[106,107,108,79,80,81];
AT(98,:)=[34,35,36,97,98,99];
%Plan brace obtuse
AT(99,:)=[91,92,93,49,50,51];
AT(100,:)=[4,5,6,100,101,102];
AT(101,:)=[94,95,96,64,65,66];
AT(102,:)=[19,20,21,103,104,105];
AT(103,:)=[97,98,99,79,80,81];
AT(104,:)=[34,35,36,106,107,108];
%Plan brace horizontal
AT(105,:)=[4,5,6,49,50,51];
AT(106,:)=[19,20,21,64,65,66];
AT(107,:)=[34,35,36,79,80,81];
%Frozen DOF's
%Base tall ver
AT(108,:)=[127,128,129,34,35,36];
AT(109,:)=[118,119,120,79,80,81];
AT(110,:)=[112,113,114,97,98,99];
AT(111,:)=[109,110,111,106,107,108];
%Base short ver
AT(112,:)=[130,131,132,43,44,45];
AT(113,:)=[124,125,126,40,41,42];
```

```
AT(114,:)=[121,122,123,88,89,90];
AT(115,:)=[115,116,117,85,86,87];
%Base brace obtuse
AT(116,:)=[127,128,129,43,44,45];
AT(117,:)=[118,119,120,88,89,90];
AT(118,:)=[112,113,114,40,41,42];
AT(119,:)=[109,110,111,85,86,87];
%Base brace acute
AT(120,:)=[109,110,111,43,44,45];
AT(121,:)=[112,113,114,88,89,90];
AT(122,:)=[118,119,120,85,86,87];
AT(123,:)=[127,128,129,40,41,42];

temp=[1,-1;-1,1];

%Calculate Lambdas and elemental stiffness matrices
for i=1:nm
    L(i)=sqrt((cm(i,4)-cm(i,1))^2+(cm(i,5)-cm(i,2))^2+(cm(i,6)-cm(i,3))^2);
    l_x(i)=(cm(i,4)-cm(i,1))/L(i);
    l_y(i)=(cm(i,5)-cm(i,2))/L(i);
    l_z(i)=(cm(i,6)-cm(i,3))/L(i);
    T(:,:,i)=[l_x(i),l_y(i),l_z(i),0,0,0;0,0,0,l_x(i),l_y(i),l_z(i)];
    k_p(:,:,i)=((A(i)*E(i))/L(i))*temp;
    k(:,:,i)=T(:,:,i)'*k_p(:,:,i)*T(:,:,i);
end

%Assemble global stiffness matrix
for ii=1:nm
    temp=AT(ii,:);
    for jj=1:nDOF_mem
        for kk=1:nDOF_mem
            K_G_temp(temp(jj),temp(kk),ii)=k(jj,kk,ii);
        end
    end
end
K_G=sum(K_G_temp,3);

%Check symmetry
K_G-K_G';

%Calculate 2D lumped-mass matrix
for i=1:108
    for j=1:108
        KK(i,j)=K_G(i,j);
    end
end

%Loads and displacements only at the main levels
n_HDOF=8;
n_Levels=3;
T=[33,36,39,99,78,81,84,108;18,21,24,96,63,66,69,105;3,6,9,93,48,51,54,102];
%External forces matrix, in N
RK=zeros(108,n_Levels);
```

```
for i=1:n_Levels
    for j=1:n_HDOF
        RK(T(i,j),i)=1/n_HDOF;
    end
end
ru=inv(KK)*RK;
m=zeros(n_HDOF,n_Levels);
for k=1:n_Levels
    for i=1:n_Levels
        for j=1:n_HDOF
            m(j,i)=ru(T(i,j),k);
        end
    end
    temp=[(sum(m(:,1))/n_HDOF);(sum(m(:,2))/n_HDOF);(sum(m(:,3))/n_HDOF)];
    F(:,k)=temp;
end
%2D lumped-mass stiffness matrix
K=inv(F);

%Loads and displacements at both main and intermediate levels
%Horizontal DoF's at main levels from bottom to top floors
n_HDOF=8;
n_Levels=3;
T=[33,36,39,99,78,81,84,108;18,21,24,96,63,66,69,105;3,6,9,93,48,51,54,102];
%External forces matrix, in N
RK=zeros(108,2*n_Levels);
ru=zeros(108,2*n_Levels);
for i=1:n_Levels
    for j=1:n_HDOF
        RK(T(i,j),(2*i))=1/n_HDOF;
    end
end
T=[45,42,90,87;30,27,75,72;15,12,60,57];
n_HDOF=4;
for i=1:n_Levels
    for j=1:n_HDOF
        RK(T(i,j),(2*i-1))=1/n_HDOF;
    end
end
%Displacements matrix
 ru=inv(KK)*RK;
%Dummy displacement, first row
ru(1,:)=0;
%Flexibility matrix
T1=[33,36,39,99,78,81,84,108;18,21,24,96,63,66,69,105;3,6,9,93,48,51,54,102];
n_HDOF=8;
T2=[45,42,90,87,1,1,1,1;30,27,75,72,1,1,1,1;15,12,60,57,1,1,1,1];
n_HDOF1=4;
m=zeros(n_HDOF,2*n_Levels);
f=zeros(2*n_Levels,2*n_Levels);
for k=1:(2*n_Levels)
    for i=1:n_Levels
        for j=1:n_HDOF
            m(j,2*i)=ru(T1(i,j),k);
```

```
            m(j,(2*i-1))=ru(T2(i,j),k);
        end
    end

temp=[(sum(m(:,1))/n_HDOF1);(sum(m(:,2))/n_HDOF);(sum(m(:,3))/n_HDOF1);(sum(m(
:,4))/n_HDOF);(sum(m(:,5))/n_HDOF1);(sum(m(:,6))/n_HDOF)];
    f(:,k)=temp;
end
%2D lumped-mass stiffness matrix
kk=inv(f);

%Flexibility matrix with loads at all levels and disp. at main levels
T=[33,36,39,99,78,81,84,108;18,21,24,96,63,66,69,105;3,6,9,93,48,51,54,102];
n_HDOF=8;
B=zeros(n_Levels, 2*n_Levels);
m=zeros(n_HDOF,n_Levels);
m1=zeros(n_HDOF,n_Levels);
for k=1:n_Levels
    for i=1:n_Levels
        for j=1:n_HDOF
            m(j,i)=ru(T(i,j),(2*k-1));
            m1(j,i)=ru(T(i,j),2*k);
        end
    end
    temp=[(sum(m(:,1))/n_HDOF);(sum(m(:,2))/n_HDOF);(sum(m(:,3))/n_HDOF)];
    temp1=[(sum(m1(:,1))/n_HDOF);(sum(m1(:,2))/n_HDOF);(sum(m1(:,3))/n_HDOF)];
    B(:,(2*k-1))=temp;
    B(:,(2*k))=temp1;
end

%Flexibility matrix with loads at main levels and disp. at all levels
T=[33,36,39,99,78,81,84,108;18,21,24,96,63,66,69,105;3,6,9,93,48,51,54,102];
n_HDOF=8;
%External forces matrix, in N
RK=zeros(108,2*n_Levels);
for i=1:n_Levels
    for j=1:n_HDOF
        RK(T(i,j),2*i)=1/n_HDOF;
    end
end
%Displacements matrix due to load at main levels
ru=inv(KK)*RK;
%Dummy displacement, first row
ru(1,:)=0;
%Flexibility matrix
T1=[33,36,39,99,78,81,84,108;18,21,24,96,63,66,69,105;3,6,9,93,48,51,54,102];
n_HDOF=8;
T2=[45,42,90,87,1,1,1,1;30,27,75,72,1,1,1,1;15,12,60,57,1,1,1,1];
n_HDOF1=4;
m=zeros(n_HDOF,2*n_Levels);
G=zeros(2*n_Levels,n_Levels);
for k=1:(n_Levels)
    for i=1:n_Levels
        for j=1:n_HDOF
```

```
            m(j,2*i)=ru(T1(i,j),(2*k));
            m(j,(2*i-1))=ru(T2(i,j),(2*k));
        end
    end

temp=[(sum(m(:,1))/n_HDOF1);(sum(m(:,2))/n_HDOF);(sum(m(:,3))/n_HDOF1);(sum(m(
:,4))/n_HDOF);(sum(m(:,5))/n_HDOF1);(sum(m(:,6))/n_HDOF)];
    G(:,k)=temp;
end


%Transformation matrices
E=kk*G;
D=K*B;
F=B*kk;
H=G*K;
```

## 2. Uncontrolled Response

```
clear all
clc

StiffnessMatrices_Transformation

%Mass matrix
ma=2*10^5;
M=eye(n_Levels,n_Levels)*ma;
D1=inv(M)*K;
lam=sort(eig(D1));
for i=1:3
    omg(i)=sqrt(lam(i));
end

MAX=7500; %MAX should be equal to the length of the longest earthquake in a,
here KOBE

ELCENTRONS_Acc; acc=acc/9.81; s=size(acc); diff(1)=MAX-s(1)*s(2); a1=[];  for
i=1:s(1); a1=[a1,acc(i,:)]; end; a(1,:)=[a1,zeros(1,diff(1))];
HACHINOHE_Acc;  acc=acc/9.81; s=size(acc); diff(2)=MAX-s(1)*s(2); a2=[];  for
i=1:s(1); a2=[a2,acc(i,:)]; end; a(2,:)=[a2,zeros(1,diff(2))];
Helena_Carroll_College_S00W_Acc;  acc=acc/9810; s=size(acc); diff(3)=MAX-
s(1)*s(2); a3=[];  for i=1:s(1); a3=[a3,acc(i,:)]; end;
a(3,:)=[a3,zeros(1,diff(3))];
Helena_Carroll_College_S90W_Acc;  acc=acc/9810; s=size(acc);  diff(4)=MAX-
s(1)*s(2); a4=[];  for i=1:s(1); a4=[a4,acc(i,:)]; end;
a(4,:)=[a4,zeros(1,diff(4))];
KOBE_Acc;  acc=acc/9.81; s=size(acc);  diff(5)=MAX-s(1)*s(2); a5=[];  for
i=1:s(1); a5=[a5,acc(i,:)]; end; a(5,:)=[a5,zeros(1,diff(5))];
Loma_Prieta_Capitola_FS_0_Acc;  acc=acc/981; s=size(acc);  diff(6)=MAX-
s(1)*s(2); a6=[];  for i=1:s(1); a6=[a6,acc(i,:)]; end;
a(6,:)=[a6,zeros(1,diff(6))];
```

```
Loma_Prieta_Capitola_FS_90_Acc;  acc=acc/981; s=size(acc);  diff(7)=MAX-
s(1)*s(2); a7=[];  for i=1:s(1); a7=[a7,acc(i,:)]; end;
a(7,:)=[a7,zeros(1,diff(7))];
Loma_Prieta_Corralito_EC_0_Acc;  acc=acc/981; s=size(acc);  diff(8)=MAX-
s(1)*s(2); a8=[];  for i=1:s(1); a8=[a8,acc(i,:)]; end;
a(8,:)=[a8,zeros(1,diff(8))];
Loma_Prieta_Corralito_EC_90_Acc;  acc=acc/981; s=size(acc); diff(9)=MAX-
s(1)*s(2); a9=[];  for i=1:s(1); a9=[a9,acc(i,:)]; end;
a(9,:)=[a9,zeros(1,diff(9))];
NORTHRIDGE_Acc;  acc=acc/9.81; s=size(acc);  diff(10)=MAX-s(1)*s(2); a10=[];
for i=1:s(1); a10=[a10,acc(i,:)]; end; a(10,:)=[a10,zeros(1,diff(10))];
Northridge_Arleta_FS_90_Acc;  acc=acc/981; s=size(acc);  diff(11)=MAX-
s(1)*s(2); a11=[];  for i=1:s(1); a11=[a11,acc(i,:)]; end;
a(11,:)=[a11,zeros(1,diff(11))];
Northridge_Arleta_FS_360_Acc;  acc=acc/981; s=size(acc);  diff(12)=MAX-
s(1)*s(2); a12=[];  for i=1:s(1); a12=[a12,acc(i,:)]; end;
a(12,:)=[a12,zeros(1,diff(12))];
Northridge_Pacoima_Dam_175_Acc;  acc=acc/981; s=size(acc);  diff(13)=MAX-
s(1)*s(2); a13=[];  for i=1:s(1); a13=[a13,acc(i,:)]; end;
a(13,:)=[a13,zeros(1,diff(13))];
Northridge_Pacoima_Dam_265_Acc;  acc=acc/981; s=size(acc);  diff(14)=MAX-
s(1)*s(2); a14=[];  for i=1:s(1); a14=[a14,acc(i,:)]; end;
a(14,:)=[a14,zeros(1,diff(14))];
NW_Cali_Ferndale_CH_N46W_Acc;  acc=acc/9810; s=size(acc);  diff(15)=MAX-
s(1)*s(2); a15=[];  for i=1:s(1); a15=[a15,acc(i,:)]; end;
a(15,:)=[a15,zeros(1,diff(15))];
NW_Cali_Ferndale_CH_S44W_Acc;  acc=acc/9810; s=size(acc);  diff(16)=MAX-
s(1)*s(2); a16=[];  for i=1:s(1); a16=[a16,acc(i,:)]; end;
a(16,:)=[a16,zeros(1,diff(16))];
Parkfield_Temblor_N65W_Acc;  acc=acc/9810; s=size(acc);  diff(17)=MAX-
s(1)*s(2); a17=[];  for i=1:s(1); a17=[a17,acc(i,:)]; end;
a(17,:)=[a17,zeros(1,diff(17))];
Parkfield_Temblor_S25W_Acc;  acc=acc/9810; s=size(acc); diff(18)=MAX-
s(1)*s(2); a18=[];  for i=1:s(1); a18=[a18,acc(i,:)]; end;
a(18,:)=[a18,zeros(1,diff(18))];
San_Fernando_1st_St_N36E_Acc;  acc=acc/981; s=size(acc);  diff(19)=MAX-
s(1)*s(2); a19=[];  for i=1:s(1); a19=[a19,acc(i,:)]; end;
a(19,:)=[a19,zeros(1,diff(19))];
San_Fernando_1st_St_N54W_Acc;  acc=acc/981; s=size(acc);  diff(20)=MAX-
s(1)*s(2); a20=[];  for i=1:s(1); a20=[a20,acc(i,:)]; end;
a(20,:)=[a20,zeros(1,diff(20))];
San_Fernando_Pac_Dam_S16E_Acc;  acc=acc/981; s=size(acc);  diff(21)=MAX-
s(1)*s(2); a21=[];  for i=1:s(1); a21=[a21,acc(i,:)]; end;
a(21,:)=[a21,zeros(1,diff(21))];
San_Fernando_Pac_Dam_S74W_Acc;  acc=acc/981; s=size(acc);  diff(22)=MAX-
s(1)*s(2); a22=[];  for i=1:s(1); a22=[a22,acc(i,:)]; end;
a(22,:)=[a22,zeros(1,diff(22))];
San_Francisco_GGP_N10E_Acc;  acc=acc/9810; s=size(acc); diff(23)=MAX-
s(1)*s(2); a23=[];  for i=1:s(1); a23=[a23,acc(i,:)]; end;
a(23,:)=[a23,zeros(1,diff(23))];
San_Francisco_GGP_S80E_Acc;  acc=acc/9810; s=size(acc); diff(24)=MAX-
s(1)*s(2); a24=[];  for i=1:s(1); a24=[a24,acc(i,:)]; end;
a(24,:)=[a24,zeros(1,diff(24))];
```

```
a=a*9.81; % Converting g's to m/s^2
T_H_unc_Hist=zeros(MAX,18);
T_H_unc_6=zeros(MAX,18);
for jj=1:24
        xg=a(jj,:);
%Check that you are using the largest acceleration data set
diff_min=min(diff);
diff_max=max(diff);

%Calculate the length of each earthquake
eq_length=MAX-diff;

t_ini=0;
dt=.02;
t_fin=((MAX)*dt)-dt;
t=t_ini:dt:t_fin;
s=size(a);

%Natural frequencies and periods
[V w]=eig(K,M);
V=fliplr(V);
w=flipud(w);
w=fliplr(w);

%Modal mass matrix
Mm=V'*M*V;

%Normalized mode shapes
for i=1:3
    V_n(:,i)=V(:,i)/sqrt(Mm(i,i));
end

%Normalized modal mass matrix
Mmm=V_n'*M*V_n;

%Modal damping
e=1.5/100;
for i=1:3
    cc(i)=2*e*Mmm(i,i)*omg(i);
end
c1=diag(cc);
c=inv(V_n')*c1*inv(V_n);
%c=zeros(3,3);
%c=1.0e+005*[2.6780,-1.1242,-0.0134;-1.1242,2.1246,-0.8851;-0.0134,-
0.8851,0.9681];
n=3;
r=3;
m=3;

%Transformation matrix
T=tril(ones(2*n,2*n));
```

```
D2=eye(n,m);
E2=eye(n,r);

Fe=diag(M)*xg;
Fc=zeros(m,MAX);

AA=[zeros(n,n),eye(n,n);-inv(M)*K,-inv(M)*c];
BB=[zeros(n,r),zeros(n,m);inv(M)*E2,inv(M)*D2];
u=[Fe;-Fc];
%CC=[eye(n,n),zeros(n,n);zeros(n,n),eye(n,n)];
%DD=zeros(2*n,2*n);

CCC=[eye(n,n),zeros(n,n);zeros(n,n),eye(n,n);-inv(M)*K,-inv(M)*c];
CC=[eye(2*n,2*n)];
%Abs acc
DDD=[zeros(2*n,2*n);zeros(n,r),inv(M)*D2];
DD=[zeros(2*n,2*n)];
%Acc rel to ground
%DD=[zeros(2*n,2*n);inv(M)*E,inv(M)*D];

sim('truss_damper_v2')

%Time-History
T_H_unc(:,:)=simout(:,:);
T_H_6_unc(:,1:6)=(inv(T)*(H*((T_H_unc(:,1:3))')))';
T_H_6_unc(:,7:12)=(H*((T_H_unc(:,4:6))'))';
T_H_6_unc(:,13:18)=(H*((T_H_unc(:,7:9))'))';
T_H_unc_Hist=T_H_unc_Hist+T_H_6_unc;


xunc_abs=[simout(:,1),simout(:,2),simout(:,3)];
xunc_drift=inv(T)*(H*xunc_abs');
xunc_d=xunc_drift';

xunc(jj,1)=max(abs(xunc_d(:,1)));
xunc(jj,2)=max(abs(xunc_d(:,2)));
xunc(jj,3)=max(abs(xunc_d(:,3)));
xunc(jj,4)=max(abs(xunc_d(:,4)));
xunc(jj,5)=max(abs(xunc_d(:,5)));
xunc(jj,6)=max(abs(xunc_d(:,6)));

acunc_abs=[simout(:,7),simout(:,8),simout(:,9)];
acunc_6=(H*acunc_abs');
acunc_66=acunc_6';

acunc(jj,1)=max(abs(acunc_66(:,1)));
acunc(jj,2)=max(abs(acunc_66(:,2)));
acunc(jj,3)=max(abs(acunc_66(:,3)));
acunc(jj,4)=max(abs(acunc_66(:,4)));
acunc(jj,5)=max(abs(acunc_66(:,5)));
acunc(jj,6)=max(abs(acunc_66(:,6)));
end
```

```
T_H_unc_avg=T_H_unc_Hist/24;
```

3. Identifying p for the various optimal design approaches

```
clear all
clc

StiffnessMatrices_Transformation
simu_run_file_66_uncontrolled
%Mass matrix
ma=2*10^5;
M=eye(n_Levels,n_Levels)*ma;
D1=inv(M)*K;
lam=sort(eig(D1));
for i=1:3
    omg(i)=sqrt(lam(i));
end

np=71;
for i=1:np
p(i)=0.9+i*0.1;
end
for ii=1:np
    for jj=1:24
        xg=a(jj,:);
%Check that you are using the largest acceleration data set
diff_min=min(diff);
diff_max=max(diff);

%Calculate the length of each earthquake
eq_length=MAX-diff;

t_ini=0;
dt=.02;
t_fin=((MAX)*dt)-dt;
t=t_ini:dt:t_fin;
s=size(a);

%Natural frequencies and periods
[V w]=eig(K,M);
V=fliplr(V);
w=flipud(w);
w=fliplr(w);

%Modal mass matrix
Mm=V'*M*V;

%Normalized mode shapes
for i=1:3
    V_n(:,i)=V(:,i)/sqrt(Mm(i,i));
end
```

```
%Normalized modal mass matrix
Mmm=V_n'*M*V_n;

%Modal damping
e=1.5/100;
for i=1:3
    cc(i)=2*e*Mmm(i,i)*omg(i);
end
c1=diag(cc);
c=inv(V_n')*c1*inv(V_n);
%c=zeros(3,3);
%c=1.0e+005*[2.6780,-1.1242,-0.0134;-1.1242,2.1246,-0.8851;-0.0134,-
0.8851,0.9681];
n=3;
r=3;
m=3;

%Transformation matrix
T=tril(ones(n,n));

D2=eye(n,m);
E2=eye(n,r);

Fe=diag(M)*xg;
Fc=zeros(m,MAX);

AA=[zeros(n,n),eye(n,n);-inv(M)*K,-inv(M)*c];
BB=[zeros(n,r),zeros(n,m);inv(M)*E2,inv(M)*D2];
u=[Fe;-Fc];
%CC=[eye(n,n),zeros(n,n);zeros(n,n),eye(n,n)];
%DD=zeros(2*n,2*n);

CCC=[eye(n,n),zeros(n,n);zeros(n,n),eye(n,n);-inv(M)*K,-inv(M)*c];
CC=[eye(2*n,2*n)];
%Abs acc
DDD=[zeros(2*n,2*n);zeros(n,r),inv(M)*D2];
DD=[zeros(2*n,2*n)];
%Acc rel to ground
%DD=[zeros(2*n,2*n);inv(M)*E,inv(M)*D];

%Optimal Damping
A=AA;
b=[zeros(n,m);inv(M)*D2];
%Energy minimization
R=inv(K);
%R=10^(-p(ii))*eye(n,n);
%Energy minimization
Q=10^(-p(ii))*[K,zeros(n,n);zeros(n,n),M];
%Remaining methods
%Q=eye(2*n,2*n);
%Q=[zeros(n,n),zeros(n,n);zeros(n,n),eye(n,n)];
```

```
%Q=[eye(n,n),zeros(n,n);zeros(n,n),zeros(n,n)];
B1=0.5*b*inv(R)*b';
C=2*Q;
P=are(A,B1,C);
%Eqn 9
G=-0.5*inv(R)*b'*P;
for i=1:n
    for j=1:n
        GX(i,j)=G(i,j);
        GXd(i,j)=G(i,j+n);
    end
end

%Equation 17 - Drift disp./vel.
Gdd=abs(GXd);
%Trnsform from 3-floor to 6-floor
gdD=E*Gdd*F;
T1=tril(ones(6,6));
gdd=T1'*gdD*T1;
%Mode shape
for i=1:n
    %Mass normalized mode shape; Mm is the modal mass
    Pp(:,i)=V(:,i)/sqrt(Mm(i,i));
end
%Mode shape from RISA for 6-floor structure; 1st mode
Del=[0.12645;0.253275;0.38585;0.51955;0.62375;0.7298];

%Scale
sc1=Pp(1,1)/Del(2,1);
sc2=Pp(2,1)/Del(4,1);
sc3=Pp(3,1)/Del(6,1);
sc=sc3;

%Mode shape from RISA scaled to actual mode shapes
Del=[0.12645;0.253275;0.38585;0.51955;0.62375;0.7298]*sc;

%Normalized drift mode shape
Del=inv(T1)*Del;
%Eqn 24, Del_c in N-sec/m
for k=1:6
   Del_n(:,1)=Del(:,1)/Del(k,1);
   Del_cd(k,1)=gdd(k,:)*Del_n;
end

sim('truss_damper_check')

x_abs=[simout(:,1),simout(:,2),simout(:,3)];
x_drift=inv(T1)*(H*(x_abs'));
x_d=x_drift';

x1(jj,ii)=max(abs(x_d(:,1)));
x2(jj,ii)=max(abs(x_d(:,2)));
x3(jj,ii)=max(abs(x_d(:,3)));
```

```
x4(jj,ii)=max(abs(x_d(:,4)));
x5(jj,ii)=max(abs(x_d(:,5)));
x66(jj,ii)=max(abs(x_d(:,6)));
x6(jj,:,ii)=[x1(jj,ii);x2(jj,ii);x3(jj,ii);x4(jj,ii);x5(jj,ii);x66(jj,ii)];

ac_abs=[simout(:,7),simout(:,8),simout(:,9)];
ac_6s=(H*(ac_abs'));
ac_6=ac_6s';

ac1(jj,ii)=max(abs(ac_6(:,1)));
ac2(jj,ii)=max(abs(ac_6(:,2)));
ac3(jj,ii)=max(abs(ac_6(:,3)));
ac4(jj,ii)=max(abs(ac_6(:,4)));
ac5(jj,ii)=max(abs(ac_6(:,5)));
ac66(jj,ii)=max(abs(ac_6(:,6)));
ac6(jj,:,ii)=[ac1(jj,ii);ac2(jj,ii);ac3(jj,ii);ac4(jj,ii);ac5(jj,ii);ac66(jj,i
i)];
    end
end
for i=1:np
    for j=1:6
        for k=1:24
            x6_RR(k,j,i)=x6(k,j,i)/xunc(k,j);
            ac6_RR(k,j,i)=ac6(k,j,i)/acunc(k,j);
        end
    end
end
for i=1:np
    x6avg(i,:)=(sum(x6_RR(:,:,i)))/24;
    ac6avg(i,:)=(sum(ac6_RR(:,:,i)))/24;
end
%First Level RR

plot(p,x6avg(:,2),p,ac6avg(:,2))
```

## 4. Identifying Δc for the performance based design

```
clear all
clc

StiffnessMatrices_Transformation
simu_run_file_66_uncontrolled
%Mass matrix
ma=2*10^5;
M=eye(n_Levels,n_Levels)*ma;
D1=inv(M)*K;
lam=sort(eig(D1));
for i=1:3
    omg(i)=sqrt(lam(i));
end

np=30;
```

```
h=50000;
del_cd(:,1)=50000*ones(6,1);
for ii=2:np
     %Average Del_cd for a range of values
    del_cd(:,ii)=del_cd(:,ii-1)+(h*ones(6,1))
end
for ii=1:np
    for jj=1:24
        xg=a(jj,:);
%Check that you are using the largest acceleration data set
diff_min=min(diff);
diff_max=max(diff);

%Calculate the length of each earthquake
eq_length=MAX-diff;

t_ini=0;
dt=.02;
t_fin=((MAX)*dt)-dt;
t=t_ini:dt:t_fin;
s=size(a);

%Natural frequencies and periods
[V w]=eig(K,M);
V=fliplr(V);
w=flipud(w);
w=fliplr(w);

%Modal mass matrix
Mm=V'*M*V;

%Normalized mode shapes
for i=1:3
    V_n(:,i)=V(:,i)/sqrt(Mm(i,i));
end

%Normalized modal mass matrix
Mmm=V_n'*M*V_n;

%Modal damping
e=1.5/100;
for i=1:3
    cc(i)=2*e*Mmm(i,i)*omg(i);
end
c1=diag(cc);
c=inv(V_n')*c1*inv(V_n);
%c=zeros(3,3);
%c=1.0e+005*[2.6780,-1.1242,-0.0134;-1.1242,2.1246,-0.8851;-0.0134,-
0.8851,0.9681];
n=3;
r=3;
m=3;
```

```
%Transformation matrix
T1=tril(ones(2*n,2*n));

D2=eye(n,m);
E2=eye(n,r);

Fe=diag(M)*xg;
Fc=zeros(m,MAX);

AA=[zeros(n,n),eye(n,n);-inv(M)*K,-inv(M)*c];
BB=[zeros(n,r),zeros(n,m);inv(M)*E2,inv(M)*D2];
u=[Fe;-Fc];
%CC=[eye(n,n),zeros(n,n);zeros(n,n),eye(n,n)];
%DD=zeros(2*n,2*n);

CCC=[eye(n,n),zeros(n,n);zeros(n,n),eye(n,n);-inv(M)*K,-inv(M)*c];
CC=[eye(2*n,2*n)];
%Abs acc
DDD=[zeros(2*n,2*n);zeros(n,r),inv(M)*D2];
DD=[zeros(2*n,2*n)];
%Acc rel to ground
%DD=[zeros(2*n,2*n);inv(M)*E,inv(M)*D];

Del_cd=zeros(6,1);
Del_cd(:,:)=del_cd(:,ii)

sim('truss_damper_check')

x_abs=[simout(:,1),simout(:,2),simout(:,3)];
x_drift=inv(T1)*(H*(x_abs'));
x_d=x_drift';

x1(jj,ii)=max(abs(x_d(:,1)));
x2(jj,ii)=max(abs(x_d(:,2)));
x3(jj,ii)=max(abs(x_d(:,3)));
x4(jj,ii)=max(abs(x_d(:,4)));
x5(jj,ii)=max(abs(x_d(:,5)));
x66(jj,ii)=max(abs(x_d(:,6)));
x6(jj,:,ii)=[x1(jj,ii);x2(jj,ii);x3(jj,ii);x4(jj,ii);x5(jj,ii);x66(jj,ii)];

v_abs=[simout(:,4),simout(:,5),simout(:,6)];
v_drift=inv(T1)*(H*(v_abs'));
v_d=v_drift';

v(jj,1)=max(abs(v_d(:,1)));
v(jj,2)=max(abs(v_d(:,2)));
v(jj,3)=max(abs(v_d(:,3)));
v(jj,4)=max(abs(v_d(:,4)));
v(jj,5)=max(abs(v_d(:,5)));
v(jj,6)=max(abs(v_d(:,6)));
```

```
fcD(:,jj)=diag(Del_cd)*v(jj,:)';

ac_abs=[simout(:,7),simout(:,8),simout(:,9)];
ac_6s=(H*(ac_abs'));
ac_6=ac_6s';

ac1(jj,ii)=max(abs(ac_6(:,1)));
ac2(jj,ii)=max(abs(ac_6(:,2)));
ac3(jj,ii)=max(abs(ac_6(:,3)));
ac4(jj,ii)=max(abs(ac_6(:,4)));
ac5(jj,ii)=max(abs(ac_6(:,5)));
ac66(jj,ii)=max(abs(ac_6(:,6)));
ac6(jj,:,ii)=[ac1(jj,ii);ac2(jj,ii);ac3(jj,ii);ac4(jj,ii);ac5(jj,ii);ac66(jj,i
i)];
    end
end
for i=1:np
    for j=1:6
        for k=1:24
            x6_RR(k,j,i)=x6(k,j,i)/xunc(k,j);
            ac6_RR(k,j,i)=ac6(k,j,i)/acunc(k,j);
        end
    end
end
for i=1:np
    x6avg(i,:)=(sum(x6_RR(:,:,i)))/24;
    ac6avg(i,:)=(sum(ac6_RR(:,:,i)))/24;
end
```

## 5. Energy Minimization

```
clear all
clc

StiffnessMatrices_Transformation
simu_run_file_uncontrolled
%Mass matrix
ma=2*10^5;
M=eye(n_Levels,n_Levels)*ma;
D1=inv(M)*K;
lam=sort(eig(D1));
for i=1:3
    omg(i)=sqrt(lam(i));
end

for ii=1
    for jj=1
        xg=a(jj,:);
%Check that you are using the largest acceleration data set
diff_min=min(diff);
diff_max=max(diff);
```

```
%Calculate the length of each earthquake
eq_length=MAX-diff;

t_ini=0;
dt=.02;
t_fin=((MAX)*dt)-dt;
t=t_ini:dt:t_fin;
s=size(a);

%Natural frequencies and periods
[V w]=eig(K,M);
V=fliplr(V);
w=flipud(w);
w=fliplr(w);

%Modal mass matrix
Mm=V'*M*V;

%Normalized mode shapes
for i=1:3
    V_n(:,i)=V(:,i)/sqrt(Mm(i,i));
end

%Normalized modal mass matrix
Mmm=V_n'*M*V_n;

%Modal damping
e=1.5/100;
for i=1:3
    cc(i)=2*e*Mmm(i,i)*omg(i);
end
c1=diag(cc);
c=inv(V_n')*c1*inv(V_n);
%c=zeros(3,3);
%c=1.0e+005*[2.6780,-1.1242,-0.0134;-1.1242,2.1246,-0.8851;-0.0134,-
0.8851,0.9681];
n=3;
r=3;
m=3;

%Transformation matrix
T=tril(ones(n,n));

D2=eye(n,m);
E2=eye(n,r);

Fe=diag(M)*xg;
Fc=zeros(m,MAX);

AA=[zeros(n,n),eye(n,n);-inv(M)*K,-inv(M)*c];
BB=[zeros(n,r),zeros(n,m);inv(M)*E2,inv(M)*D2];
```

```
u=[Fe;-Fc];

CCC=[eye(n,n),zeros(n,n);zeros(n,n),eye(n,n);-inv(M)*K,-inv(M)*c];
CC=[eye(2*n,2*n)];
%Abs acc
DDD=[zeros(2*n,2*n);zeros(n,r),inv(M)*D2];
DD=[zeros(2*n,2*n)];

%Optimal Damping
A=AA;
b=[zeros(n,m);inv(M)*D2];
%Energy minimization
R=inv(K);
Q=10^(-2.65)*[K,zeros(n,n);zeros(n,n),M];
B1=0.5*b*inv(R)*b';
C=2*Q;
P=are(A,B1,C);
%Eqn 9
G=-0.5*inv(R)*b'*P;
for i=1:n
    for j=1:n
        GX(i,j)=G(i,j);
        GXd(i,j)=G(i,j+n);
    end
end

%Equation 17 - Drift disp./vel.
Gdd=abs(GXd);
%Trnsform from 3-floor to 6-floor
gdD=E*Gdd*F;
T1=tril(ones(6,6));
gdd=T1'*gdD*T1;
%Mode shape
for i=1:n
    %Mass normalized mode shape; Mm is the modal mass
    Pp(:,i)=V(:,i)/sqrt(Mm(i,i));
end
%Mode shape from RISA for 6-floor structure; 1st mode
Del=[0.12645;0.253275;0.38585;0.51955;0.62375;0.7298];

%Scale
sc1=Pp(1,1)/Del(2,1);
sc2=Pp(2,1)/Del(4,1);
sc3=Pp(3,1)/Del(6,1);
sc=sc3;

%Mode shape from RISA scaled to actual mode shapes
Del=[0.12645;0.253275;0.38585;0.51955;0.62375;0.7298]*sc;

%Normalized drift mode shape
Del=inv(T1)*Del;
%Eqn 24, Del_c in N-sec/m
for k=1:6
```

```
   Del_n(:,1)=Del(:,1)/Del(k,1);
   Del_cd(k,1)=gdd(k,:)*Del_n;
end

sim('truss_damper_check')

x_abs=[simout(:,1),simout(:,2),simout(:,3)];
x_drift=inv(T1)*(H*(x_abs'));
x_d=x_drift';

x1(jj,ii)=max(abs(x_d(:,1)));
x2(jj,ii)=max(abs(x_d(:,2)));
x3(jj,ii)=max(abs(x_d(:,3)));
x4(jj,ii)=max(abs(x_d(:,4)));
x5(jj,ii)=max(abs(x_d(:,5)));
x66(jj,ii)=max(abs(x_d(:,6)));
x6(jj,:,ii)=[x1(jj,ii);x2(jj,ii);x3(jj,ii);x4(jj,ii);x5(jj,ii);x66(jj,ii)];

v_abs=[simout(:,4),simout(:,5),simout(:,6)];
v_drift=inv(T1)*(H*(v_abs'));
v_d=v_drift';

v1(jj,ii)=max(abs(v_d(:,1)));
v2(jj,ii)=max(abs(v_d(:,2)));
v3(jj,ii)=max(abs(v_d(:,3)));
v4(jj,ii)=max(abs(v_d(:,4)));
v5(jj,ii)=max(abs(v_d(:,5)));
v66(jj,ii)=max(abs(v_d(:,6)));

v6(jj,:,ii)=[v1(jj,ii);v2(jj,ii);v3(jj,ii);v4(jj,ii);v5(jj,ii);v66(jj,ii)];

fcD(:,jj)=diag(Del_cd)*v6(jj,:,:)';

ac_abs=[simout(:,7),simout(:,8),simout(:,9)];
ac_6s=(H*(ac_abs'));
ac_6=ac_6s';

ac1(jj,ii)=max(abs(ac_6(:,1)));
ac2(jj,ii)=max(abs(ac_6(:,2)));
ac3(jj,ii)=max(abs(ac_6(:,3)));
ac4(jj,ii)=max(abs(ac_6(:,4)));
ac5(jj,ii)=max(abs(ac_6(:,5)));
ac66(jj,ii)=max(abs(ac_6(:,6)));
ac6(jj,:,ii)=[ac1(jj,ii);ac2(jj,ii);ac3(jj,ii);ac4(jj,ii);ac5(jj,ii);ac66(jj,i
i)];
    %Abs. force
 Fcontrol(:,jj)=inv(T1')*fcD(:,jj);
    end
end
for i=1
    for j=1:6
        for k=1
```

```
            x6_RR(k,j,i)=x6(k,j,i)/xunc(k,j);
            ac6_RR(k,j,i)=ac6(k,j,i)/acunc(k,j);
        end
    end
end
Del_cd
x6_RR
ac6_RR
sum(fcD,2);
%Time History
T_H(:,:)=simout(:,:);
T_H_6(:,1:6)=(inv(T1)*(H*((T_H(:,1:3))')))';
T_H_6(:,7:12)=(H*((T_H(:,4:6))'))';
T_H_6(:,13:18)=(H*((T_H(:,7:9))'))';
```

## 6. S-Function

```
function [sys,x0,str,ts] = simu66(t,x,u,flag,Del_cd)
%sys=u

switch flag,
  case 0
    [sys,x0,str,ts]=mdlInitializeSizes;

  case 3
    sys=mdlOutputs(t,x,u,Del_cd);

  case { 1, 2, 4, 9 }
    sys=[];

  otherwise
    error(['Unhandled flag = ',num2str(flag)]);

end

function [sys,x0,str,ts] = mdlInitializeSizes()

sizes = simsizes;
sizes.NumContStates  = 0;
sizes.NumDiscStates  = 0;
sizes.NumOutputs     = [6];  % dynamically sized
sizes.NumInputs      = [6];  % dynamically sized
sizes.DirFeedthrough = 1;   % has direct feedthrough
sizes.NumSampleTimes = 1;

sys = simsizes(sizes);
str = [];
x0  = [];
ts  = [-1 0];   % inherited sample time

function sys = mdlOutputs(t,x,u,Del_cd)
```

```
%From my code
T1=tril(ones(6,6));
H=[0.49580056507907,0.00219930141859,-
0.00021838890332;1.00000000000000,0.00000000000000,-
0.00000000000000;0.49799986649766,0.49806116429239,0.00173808629907;-
0.00000000000000,1.00000000000000,-
0.00000000000000;0.00198091251527,0.49781833807620,0.50032036118723;-
0.00000000000000,0.00000000000000,1.00000000000000];
D=H';

v(1,1)=u(4,1);
v(2,1)=u(5,1);
v(3,1)=u(6,1);

%Rel to ground vel
v1=v(1,1);
v2=v(2,1);
v3=v(3,1);

Vel=[v1;v2;v3];

vel=H*Vel;
%Drift Velocity
vel_D=inv(T1)*vel;

%Optimal del_c
fc_D=diag(Del_cd)*vel_D;

%Abs. force
fc=inv(T1')*fc_D;

FC=D*fc;
u=[0;0;0;-FC];

sys = u;
```

## NOMENCLATURE

| | |
|---|---|
| $N$ | DOF of 3D truss tower model |
| $N$ | DOF of equivalent 2D lumped mass model |
| $\ddot{\mathbf{X}}(t)$ | Relative to ground acceleration for $N$DOF 2D lumped mass model |
| $\dot{\mathbf{X}}(t)$ | Relative to ground velocity for $N$DOF 2D lumped mass model |
| $\mathbf{X}(t)$ | Relative to ground displacement for $N$DOF 2D lumped mass model |
| $\mathbf{M}$ | Mass matrix for $N$DOF 2D lumped mass model |
| $\mathbf{C}$ | Damping matrix for $N$DOF 2D lumped mass model |
| $\mathbf{K}$ | Stiffness matrix for $N$DOF 2D lumped mass model |
| $\mathbf{D}$ | Location matrix for control forces |
| $\mathbf{U}(t)$ | Control forces |
| $m$ | Number of control devices for $N$DOF system |
| $\ddot{X}_g(t)$ | Seismic ground acceleration |
| $\dot{\mathbf{z}}(t)$ | Time derivative of the states of the $N$DOF system |
| $\mathbf{z}(t)$ | States of the $N$DOF system |
| $\mathbf{A}$ | System matrix for the $N$DOF system |
| $\mathbf{B}$ | Input location matrix for control forces for $N$DOF system |
| $\mathbf{H}$ | Input location matrix for earthquake forces for $N$DOF system |

| | |
|---|---|
| $\delta$ | Flexibility coefficient |
| $J$ | Performance index |
| $\mathbf{Q}$ | Weighing matrix for states of the structure |
| $\mathbf{R}$ | Weighing matrix for the control forces on the structure |
| $\mathbf{G}$ | Gain matrix for the *N*DOF system |
| $\mathbf{G}_x$ | Relative to ground displacement gain matrix for the *N*DOF system |
| $\mathbf{G}_{\dot{x}}$ | Relative to ground velocity gain matrix for the *N*DOF system |
| $\mathbf{P}$ | Solution of the ARE equation |
| $\mathbf{T}_N$ | Lower-diagonal unity transformation matrix for *N*DOF system |
| $\mathbf{G}_{\dot{d}}$ | Interstory drift velocity gain matrix for the *N*DOF system |
| $\mathbf{\Delta C}_d$ | Diagonal damping coefficient matrix for the *N*DOF system |
| $\mathbf{\Phi}_d$ | Normalized drift mode shapes for the *N*DOF system |
| $\mathbf{\Delta c}_d$ | Diagonal damping coefficient matrix for the *n*DOF system |
| $\mathbf{g}_{\dot{d}}$ | Interstory drift velocity gain matrix for the *n*DOF system |
| $\boldsymbol{\phi}_d$ | Normalized drift mode shapes for the *n*DOF system |
| $\mathbf{T}_n$ | Lower-diagonal unity transformation matrix for *n*DOF system |
| $\boldsymbol{\phi}$ | Normalized mode shapes for the *n*DOF system |
| $\mathbf{S}$ | Transformation matrix |

| | |
|---|---|
| $\mathbf{V}$ | Transformation matrix |
| $\mathbf{\Phi}$ | Normalized mode shapes for the *N*DOF system |
| $\mathbf{F}$ | Flexibility matrix |
| $\mathbf{E}$ | Flexibility matrix |
| $l$ | Number of control devices for *n*DOF system |
| $\mathbf{f}_{cd}(t)$ | Control force in drift form for *n*DOF system |
| $\dot{\mathbf{x}}_d(t)$ | Inter story drift velocity for *n*DOF system |
| $\dot{\mathbf{x}}(t)$ | Relative to ground velocity for *n*DOF system |
| $\mathbf{f}_c(t)$ | Relative to ground control force for *n*DOF system |
| $\mathbf{F}_c(t)$ | Relative to ground control force for *N*DOF system |
| $\mathbf{L}$ | Transformation matrix |
| $\mathbf{W}$ | Flexibility matrix |

## REFERENCES


[1] M. D. Symans and M. C. Constantinou, "*Semi-active control systems for seismic protection of structures: a state-of-the-art review*", Engineering Structures, Vol. 21, 469-487, Elsevier 1999.

[2] M. D. Symans and M. C. Constantinou, "*Passive fluid viscous damping systems for seismic energy dissipation*", ISET Journal of Earthquake Technology, Paper no. 382, Vol. 35 No.4, 185-206, 1998.

[3] T. T. Soong and G. F. Dargush, "*Passive energy dissipation system in structural engineering*", Wiley 1997.

[4] R. J. McNamara and D. P. Taylor, "*Fluid viscous dampers for high-rise buildings*". The Structural Design of Tall and Special Buildings, Vol. 12 Issue 2, 145-154, Wiley 2003.

[5] F. Sadek, B. Mohraz, A. W. Taylor and R. M. Chung, "*Passive energy dissipation devices for seismic applications*", Building and Fire Research Laboratory, Maryland 1996.

[6] H. C. Huang and R. J. McNamara, "*The efficiency of motion amplification device with viscous damper*".

[7] M. C. Constantinou, P. Tsopelas, W. Hammel and A. N. Sigaher, "*Toggle-brace-damper seismic energy dissipation systems*", Journal of Structural Engineering, Vol. 127, No. 2, 105-112, ASCE 2001.

[8] D. P. Taylor, "*Toggle brace dampers: A new concept for structural control*", Advanced Technology in Structural Engineering: Proceedings, Strcutures Congress and Exposition 2000.

[9] K. R. Raju, A. M. Prasad, N. Lakshmanan, K. Muthumani, D. R. Jagadish and R. Amuthasheela, "*Optimum distribution of viscous fluid dampers in structural systems*", Institute of Engineers (India) Journal, Vol. 86, 103-108, 2005.

[10] Y. Ribakov and A. M. Reinhorn, "*Design of amplified structural damping using optimal considerations*" Journal of Structural Engineering, Vol. 129, No. 10, 1422-1427, ASCE 2003.

[11] J. Jiuhong, D. Jianye, W. Yu and H. Hongxing, "*Design method for fluid viscous dampers*", Archives of Applied Mechanics, Vol. 78, 737-746, Springer 2008.

[12] T. Murakami, M. Sakai and M. Nakano, "*Experimental evaluation of a passive type MR fluid damper*".

[13] W. L. He and A. K. Agarwal, "*Energy transfer approach for the design of passive energy dissipation systems*", 15th ASCE Engineering Mechanics Conference, Columbia University 2002.

[14] A. K. Agarwal and J. N. Yang, "*Design of passive energy dissipation systems based on LQR control methods*", Journal of Intelligent Material Systems and Structures, Vol. 10, 933-944, Technomic 2000.

[15] N. Gluck, A. M. Reinhorn, J. Gluck and R. Levy, "*Design of supplemental dampers for control of structures*", Journal of Structural Engineering, Vol. 122, No. 12, 1394-1399, ASCE 1996.

[16] W. L. Qu, Z. H. Chen and Y. L. Xu, "*Dynamic analysis of wind-excited truss tower with friction dampers*", Computers and Structures, Vol. 79, 2817-2831, Pergamon 2001.

[17] J. W. Tedesco, W. G. McDougal and C. A. Ross, "*Structural dynamics theory and applications*", Addison Wesley 1998.

[18] R. C. Hibbeler, "*Structural analysis*", Prentice Hall 2005.

[19] F. Sadek and B. Mohraz, "*Semiactive control algorithms for structures with variable dampers*", Journal of Engineering Mechanics, Vol. 124, No. 9, 981-990, ASCE 1998.

## BIOGRAPHICAL SKETCH

Sujatha Kalyanam

In the spring of 2002, Sujatha Kalyanam graduated with a bachelor's degree in civil engineering from Madras University, India. She then obtained a master's degree in engineering mechanics under the guidance of Dr. Eveline Baesu from the University of Nebraska-Lincoln in spring of 2005. She will be graduating with a master's degree in civil engineering from Florida State University in summer of 2009. She conducted research under the guidance of Dr. Michelle Rambo-Roddenberry and Dr. Ken Walsh. Her research interest lies in structural engineering, particularly concrete and steel design.